Peli1 facilitates virus replication and promotes neuroinflammation during West Nile virus infection

Huanle Luo [1, +], Evandro R Winkelmann [1, +], Shuang Zhu [2], Wenjuan Ru [3], Elizabeth Mays [1], Jesus A Silvas [4], Lauren L Vollmer [5], Junling Gao [3], Bi-Hung Peng [3], Nathen E Bopp [4], Courtney Cromer [4], Chao Shan [6], Guorui Xie [1], Guangyu Li [1], Robert Tesh [4, 7], Vsevolod L Popov [4,7], Pei-Yong Shi [6, 7], Shao-Cong Sun [8], Ping Wu [3,7], Robyn S Klein [5], Shao-Jun Tang [3,7], Wenbo Zhang [2, 3, 7], Patricia V. Aguilar [4, 7], and Tian Wang [1, 4, 7, *]

[1]Department of Microbiology & Immunology, University of Texas Medical Branch, Galveston, TX, 77555, USA. [2]Department of Ophthalmology and Visual Sciences, University of Texas Medical Branch, Galveston, TX, 77555, USA. [3]Department of Neuroscience, Cell Biology and Anatomy, University of Texas Medical Branch, Galveston, TX, 77555, USA. [4]Department of Pathology, University of Texas Medical Branch, Galveston, TX, 77555, USA. [5]Department of Medicine, Washington University School of Medicine, St. Louis, MO 63110, USA. [6]Department of Biochemistry & Molecular Biology, University of Texas Medical Branch, Galveston, TX, 77555, USA. [7]Institute for Human Infections & Immunity, University of Texas Medical Branch, Galveston, TX, 77555, USA. [8]Department of Immunology, The University of Texas MD Anderson Cancer Center, Houston, Texas, USA.

[+] These authors contributed equally to this work

[*] Address correspondence to: Tian Wang, Departments of Microbiology & Immunology and Pathology, University of Texas Medical Branch, Keiller 3.118B, 301 University Boulevard, Galveston, TX, 77555-0609, USA. Telephone: +1-409-772-3146; E-mail: ti1wang@utmb.edu

Figures: 8; Supplemental Figures: 7; Supplemental Table: 1

Running Title: Peli1 facilitates West Nile virus replication

Abstract:

The E3 ubiquitin ligase - Pellino (Peli)1 is a microglia-specific mediator of autoimmune encephalomyelitis. Its role in neurotropic flavivirus infection is largely unknown. Here, we report that mice deficient of Peli1 (*Peli1*$^{-/-}$) were more resistant to lethal West Nile virus (WNV) infection and exhibited reduced viral loads in tissues and attenuated brain inflammation. Peli1 mediates chemokine and proinflammatory cytokine production in microglia and promotes T cells and macrophages infiltration into the central nervous system. Unexpectedly, Peli1 was required for WNV entry and replication in mouse macrophages, and mouse and human neurons and microglia. It was also highly expressed on WNV-infected neurons and adjacent inflammatory cells in acute post-mortem WNV encephalitis patients. WNV- passaged in *Peli1*$^{-/-}$ macrophages or neurons induced a lower viral load and impaired activation in wild-type microglia thereby a reduced lethality in mice. Smaducin-6, which blocks interactions between Peli1 to IRAK1, RIP1, and IKKε did not inhibit WNV-triggered microglia activation. Collectively, our findings suggest a non- immune regulator role of Peli1 in promoting microglia activation during WNV infection and identify a potential novel host factor for flavivirus cell entry and replication.

INTRODUCTION

Pellino (Peli)1, an E3 ubiquitin ligase, is an important regulator in innate and adaptive immunity. It is essential for nuclear factor (NF)-κB activation induced by TIR-domain-containing, adapter-inducing interferon-β (TRIF)/toll-like receptor (TLR)-mediated signaling in innate immune cells such as macrophages and dendritic cells (DCs) (1). In microglial cells, where Peli1 is predominantly expressed in the brain, it regulates TLR/MyD88 signaling by promoting degradation of TNF receptor-associated factor 3 (Traf3), a process which leads to microglia activation during the course of induction of experimental autoimmune encephalomyelitis (EAE) (2). Peli1 is also implicated in regulation of adaptive immune cell functions. For example, it is a critical factor in the maintenance of peripheral T cell tolerance by regulating c-Rel via its K48 ubiquitination (3). Peli1 upregulation plays a role in B cell lymphomas tumorigenesis (4).

West Nile virus (WNV), a mosquito-borne, single-stranded flavivirus that caused outbreaks in Asia, Europe, and Australia, has been the leading cause of viral encephalitis in the United States (US) for more than one decade (5, 6). The features of acute illness range from WN fever to neuroinvasive conditions, including meningitis, encephalitis, acute flaccid paralysis, and death (7). In addition, up to 50% of WNV convalescent patients have been reported to have long-term neurological sequelae or chronic kidney disease (8-16). Currently, there is no specific therapeutic agent for treatment of WNV infection, and an approved vaccine is not available for humans. Studies in animal models suggest that WNV-induced central nervous system (CNS) disease is caused by neuronal degeneration, a direct result of viral infection, and/or by bystander damage from the immune response to the pathogen in the CNS (17, 18) that is induced by infiltrating inflammatory cells and CNS resident cells, including microglia/macrophages, neutrophils, and lymphocytes (19-23). Microglial cells, the resident macrophages of the CNS that express various pattern recognition receptors (PRRs), become activated and produce innate proinflammatory molecules upon encountering microbial infection. Microglia activation in the CNS is the hallmark of acute WNV- infection (24, 25). It was also

shown to drive neuronal and synaptic loss which together contributes to memory impairment in WNV-induced chronic cognitive sequelae (26). The underlying immune mechanisms of microglia activation are not clearly understood. Here, we hypothesize that Peli1 mediates the activation of microglia and promotes neuroinflammation during lethal WNV infection. Unexpectedly, we found that Peli1 is required for WNV entry and replication in both peripheral myeloid cells and CNS resident cells. In particular, a defective WNV replication in Peli1-deficient microglia and neurons directly contributes to attenuated neuroinflammation in the CNS and ultimately decreases host susceptibility to lethal encephalitis.

RESULTS

Peli1$^{-/-}$ mice were more resistant to systemic WNV infection.

Peli1 promotes microglia-mediated brain inflammation in the course of EAE induction (2). To investigate the role of Peli1 in WNV encephalitis, we infected WT and *Peli1*$^{-/-}$ mice i.p. with 100 FFU WNV 385-99 strain and monitored daily for survival (Figure 1A). *Peli1*$^{-/-}$ mice (39% survival) were more resistant to WNV infection than WT controls (9.5% survival). To further understand viral pathogenesis, we measured viral burden in the peripheral organs and brain. *Peli1*$^{-/-}$ mice had lower viremia at days 2 and 3 post infection (pi) and decreased splenic viral load at day 6 compared to WT mice (Figure 1, B and C). WNV crosses the blood brain barrier (BBB) and infects the CNS around day 3 in mice (25). Viral RNA levels in *Peli1*$^{-/-}$ mouse brains were more than 15–fold lower than that of WT mice at day 6 pi (Figure 1D). This trend continued but became insignificant at day 9 when both groups of mice started to succumb to lethal WNV infection. On day 6 pi, meningitis (inflammation of the leptomeninge) was noted in WT mice, but not in *Peli1*$^{-/-}$ mice (Figure 1E). Inflammation further spread to the brain parenchyma (encephalitis) as seen in striatum, hippocampus, and cerebellum in both groups of mice at day 9. Encephalitis, particularly perivascular cuffing and microglia activation (cells with elongated nuclei), was much more extensive in WT mice. Thus, CNS inflammation started earlier and was more severe in WNV-infected WT mice compared to *Peli1*$^{-/-}$ mice. No histopathology differences were noted in naïve mouse brains between WT and *Peli1*$^{-/-}$ groups (Supplemental Figure 1).

Peli1$^{-/-}$ mice exhibited impaired innate cytokine production, but modestly enhanced adaptive immune responses in the periphery.

Peli1 is known to facilitate TRIF-dependent TLR signaling and proinflammatory cytokine production (1). Following WNV infection, Peli1 expression was increased in the blood of WT mice (Supplemental Figure 2A). The RNA levels of interferon (*Ifn*)*a* and *Ifnb* at day 6,

interleukin (*Il)6*, tumor necrosis factor (*Tnf*)*a* at days 3 and 6, and *Il12* at day 3 were all diminished in *Peli1*$^{-/-}$ mice (Supplemental Figure 2B). The blood plasma protein levels of IL-1β and IL-10 were also reduced in *Peli1*$^{-/-}$ mice (Supplemental Table 1), though no differences were noted in plasma IFN-γ and IL-17 levels between the two groups of mice. To study adaptive immune responses in the periphery, we first measured antibody production in the blood. WNV -specific IgM responses were modestly enhanced in *Peli1*$^{-/-}$ mice at days 3 and 9 pi (Supplemental Figure 2C). WNV-specific IgG responses were similar between the two groups of mice (Supplemental Figure 2D). Peli1 is also known to negatively regulate T cell signaling (3). We next collected the spleen tissues from naive and WNV infected WT and *Peli1*$^{-/-}$ mice. No necrosis was observed in any of the spleen sections examined. There was a trend of the white pulp expansion resulting from germinal center proliferation in WT group at days 3 and 6 pi, but returned to similar levels as naive mice at day 9; in *Peli1*$^{-/-}$ mice the expansion was continuously enhanced (Supplemental Figure 2, E and F). On day 7, both splenic CD4$^+$ and CD8$^+$ T cells of *Peli1*$^{-/-}$ mice produced more IFN-γ than WT mice upon *ex vivo* re-stimulation with WNV-specific peptides. CD4$^+$ T cells of *Peli1*$^{-/-}$ mice also induced higher IL-6 and IL-10 production (Supplemental Figure 2, G and H).

Peli1 was required for WNV entry and viral replication in macrophages and dendritic cell (DC)s which further activated innate cytokine responses.

Macrophages and DCs are innate immune cells expressing many PRRs and both cell types are permissive to WNV infection in the peripheral organs (27). To study Peli1-mediated innate immune responses upon WNV infection, we first measured viral loads in these two cell types by quantitative (q)PCR and focus-forming assays (FFA) and found that both viral RNA levels and viral titers were significantly diminished in primary myeloid *Peli1*$^{-/-}$ macrophages and DCs compared to WT controls (Figure 2, A and B and Supplemental Figure 3, A and B). We

next performed virus attachment and entry assays to determine Peli1 involvement in the WNV replication cycle. Macrophages of both groups were incubated with WNV (MOI of 3 or 10) at 4°C for 1 h, allowing the virus to attach to the cell surface. After 1 h incubation, the cells were washed to remove unattached virus, and the amounts of viruses that had attached to the cell surface were measured by qPCR. It was noted that *Peli1*$^{-/-}$ macrophages attached 28% less virus than the WT cells (Figure 2C). Cells were further incubated at 37°C to initiate viral entry. At 1.5 h and 5 h pi, the infected cells were stringently washed to remove free virus as well as cell surface-associated virus, and the intracellular viral RNA was quantified. As shown in Figure 2D, levels of viral RNA in *Peli1*$^{-/-}$ macrophages were 27% to 54% lower than those of WT cells. These results indicated that Peli1 is involved in WNV attachment and entry. To confirm these results, we performed ultrastructural analysis of macrophages of both groups at 0 min, 5 min, and 10 h after exposure to WNV (Figure 2, E and F). At 0 h, we observed 16 WNV particles ranging between 41 to 46 nm in diameter associated with the plasma membrane in WT macrophages; whereas a total of 7 WNV particles were found in association with the plasma membrane of *Peli1*$^{-/-}$ macrophages. At 5 m pi, 38 viral particles with a diameter of about 42 nm were noted in small uncoated vesicles of WT macrophages**.** However, only 11 WNV particles with the same size were identified in *Peli1*$^{-/-}$ macrophages. By 10 h, there were 55 WNV viral particles with a diameter of 42 nm inside the double membrane vesicles of WT macrophages. Interestingly, 18 viral particles with much smaller size (about 25 nm) were found inside the double membrane vesicles of *Peli1*$^{-/-}$ macrophages (Figure 2, E-F). At day 4 pi, virus particles detected in the supernatants of WT macrophages ranged in diameter from 41 nm to 47 nm, which are in similar dimensions to those previously reported (28); whereas virions detected in the supernatant of the *Peli1*$^{-/-}$ macrophages showed significant variations in size ranging from 23.5 nm to 39.5 nm (Figure 2G). These observations suggest that Peli1 not only plays a role in the initial cell attachment and entry, but also in other aspects of WNV life cycle within the host cells. We next determined the infectivity of WNV that was passaged in WT or *Peli1*$^{-/-}$

159 macrophages. WNV passaged in *Peli1*$^{-/-}$ macrophages had a lower replication rate in WT
160 macrophages versus WNV passage in WT cells (Figure 2H). Furthermore, we challenged WT
161 and *Peli1*$^{-/-}$ mice with 100 FFU of WNV passaged in WT or *Peli1*$^{-/-}$ macrophages. WT mice
162 infected with WNV passaged in *Peli1*$^{-/-}$ macrophages showed an increased survival rate
163 (28.5%, Figure 2I) compared to WT mice infected with WNV passaged in WT cells (0%).
164 *Peli1*$^{-/-}$ mice infected with WNV passaged either in WT macrophages (43%) or *Peli1*$^{-/-}$ cells
165 (56%) also showed similar resistance to lethal WNV infection.
166 We next determined if Peli1 mediated immune responses during WNV infection in
167 macrophages and DCs. Following WNV infection, *Peli1* expression was upregulated in
168 macrophages at day 4. In contrast, the other two Pellino family members, including *Peli2* and
169 *Peli3*, remained at low levels (Figure 3A). Compared to WT cells, *Peli1*$^{-/-}$ macrophages had
170 reduced *Ifna* and *Ifnb* RNA levels at days 1 and 4 after WNV infection (Figure 3, B and C).
171 Production of inflammatory cytokines, including IL-6, TNF-α, and IL-12, was also impaired in
172 *Peli1*$^{-/-}$ macrophages at day 4 (Figure 3, D-F). WNV infection in *Peli1*$^{-/-}$ DCs also resulted in
173 diminished levels of *Ifnb*, *Il1b*, and *Il12* compared to WT DCs (Supplemental Figure 3C). PRRs,
174 including TLR3, TLR7, and retinoid acid-inducible gene-I (RIG-I) –like receptor (RLR)s, such as
175 RIG-I and melanoma differentiation antigen 5 (MDA-5), are involved in WNV recognition and
176 trigger the signaling cascade leading to the production of type 1 IFNs and pro-inflammatory
177 cytokines (25, 29-31). To understand the role of Peli1 in PRR-mediated signaling pathways, we
178 treated WT and *Peli1*$^{-/-}$ macrophages with TLR agonists (Poly I:C for TLR3, CL097 for TLR7,
179 and Poly I:C LyoVec for RLRs). Both Poly I:C or Poly I:C/LyoVec triggered lower *Ifna*, *Ifnb*, *Il6*,
180 and *Il12* levels in *Peli1*$^{-/-}$ macrophages. In contrast, stimulation with TLR7 agonist induced
181 similar antiviral cytokine responses in both groups of macrophages (Supplemental Figure 3, D-
182 G). Peli1 is known to be dispensable for MyD88-dependent TLRs, but is required for TRIF-
183 dependent TLR signaling in macrophages and DCs (1). Consistent with the previous findings,
184 we demonstrate that Peli1 positively regulates TLR3 and RLR but not TLR7 -mediated innate

cytokine responses in macrophages. Finally, to understand the effects of defective viral replication on antiviral immunity, we infected WT macrophages with the same dose of WNV passaged once in WT or *Peli1*$^{-/-}$ macrophages. Interestingly, WNV passaged in *Peli1*$^{-/-}$ cells triggered diminished *Ifnb* RNA and IL-6 protein levels in WT macrophages compared to those isolated from WT cells. The levels of reduction induced by WNV passaged in *Peli1*$^{-/-}$ cells were similar to WT virus induced in *Peli1*$^{-/-}$ cells (Figure 3G and Supplemental Figure 3H). Collectively, these data show that Peli1 positively mediates antiviral cytokine responses mainly by a direct involvement in WNV replication life cycle in macrophages and DCs.

Peli1 was predominantly involved in CNS inflammation during WNV infection

Peli1 was previously reported to be highly expressed by neural tissues (2). Here, we noted *Peli1* expression was induced in the brain on days 6 and 9 pi (Figure 4A). The mRNA levels of inflammatory cytokines including *Il1b*, *Il6*, and *Tnfa* and chemokines such as *Ccl2*, *Ccl7*, and *Cxcl10* were decreased in *Peli1*$^{-/-}$ mice (Figure 4B-G). *Ifnb* but not *Ifna* RNA levels were also reduced in *Peli1*$^{-/-}$ mouse brains (Supplemental Figure 4, A and B). To study brain leukocyte phenotype, we performed flow cytometry analysis of these cells isolated at day 9 and found that the number and the percentage of infiltrating $CD4^+$ T cells, activated microglial cells ($CD11b^{hi}CD45^{lo}$), and macrophages ($CD11b^{hi}CD45^{hi}$) were decreased up to 60% in *Peli1*$^{-/-}$ mice (Figure 4, H-I & Supplemental Figure 4C). To exclude the effects of Peli1 on WNV infection in the periphery tissues, we inoculated WNV intracranially (i.c.) into both groups of mice (Figure 4J). *Peli1*$^{-/-}$ mice showed a similar resistance as in systemic WNV infection (44% versus 11%, *Peli1*$^{-/-}$ versus WT). Collectively, these results indicate that Peli1 is involved in WNV encephalitis predominantly by mediating CNS infection and induction of neuroinflammation.

Peli1 promoted microglia activation via facilitating WNV replication in neurons and microglia in mice and humans.

Microglial cells are involved in CNS neuroinflammation (24, 32) and are permissive to WNV infection (Supplemental Figure 5A). *Peli1* is highly expressed on microglial cells (2) and was enhanced following WNV infection, however, *Peli2* and *Peli3* remained at low levels (Figure 5A and Supplemental Figure 5B). WNV triggered higher mRNA levels of inflammatory cytokines (*Tnfa* and *Il12*) and chemokines (*Ccl2*, *Ccl4*, and *Cxcl10*) in microglial cells (Supplemental Figure 5C). Interestingly, WNV infection was nearly abolished in both *Peli1*$^{-/-}$ primary microglial cells (Figure 5, B and C) and Peli1-depleted microglial cells (Supplemental Figure 5D), which was accompanied by diminished levels of inflammatory cytokines and chemokines (Figure 5D and Supplemental Figure 5E). Neurons are most permissive to WNV infection in the CNS (18, 33). WNV infection upregulates *Peli1* expression on neurons up to 200% (Figure 5E). WNV replication was also significantly reduced in *Peli1*$^{-/-}$ neurons compared to WT neurons (Figure 5, F and G). The mRNA levels of chemokines (*Ccl2*, *Ccl7*, *Cxcl10*), inflammatory cytokine (*Il6*), and *Ifnb* were all diminished in WNV-infected *Peli1*$^{-/-}$ neurons at day 4 (Figure 5H, and Supplemental Figure 5F). Western blot analysis showed that the phosphorylation levels of p38MAPK and p65 were both reduced in WNV- infected *Peli1*$^{-/-}$ neurons at day 3 compared to WT controls (Supplemental Figure 5, G and H) which suggests a role of Peli1 in positive regulation of NF-κB and p38MAPK activation.

Immunostaining of acute post-mortem WNV encephalitis patient hippocampal tissues show membrane Peli1 on WNV- positive neurons and adjacent inflammatory cells, but not in the same region of the age-match patient controls (Figure 6A). *Peli1* expression was also upregulated following in vitro WNV infection in SHSY-5Y- differentiated neurons and HMC3 cells (human microglial cell line (Figure 6, B and C) and WNV- infected PBMCs (Supplemental Figure 6A). Nevertheless, its expression was not changed in WNV-infected neural stem cell- derived neurons nor THP1- derived macrophages (Supplemental Figure 6A). Knockdown of Peli1

expression on human microglial cells or SHSY-5Y- differentiated neurons decreased viral loads by 20- 35% at day 4 pi (Figure 6, D and E and Supplemental Figure 6B). Peli1 deficiency also decreased IL-6, CCL2 and CCL5 production in human microglial cells (Figure 6, F-H). WNV infection did not induce inflammatory cytokine or chemokine production in human neurons (data not shown). It was noted that *Peli1* knockdown (36% reduction, Supplemental Figure 6C) in human fetal cortical neural stem cells (hNSCs)- derived neurons led to a 30% decrease on *Ifnb* levels at day 4 pi compared to control-siRNA- treated neurons (Supplemental Figure 6D). These data suggests that Peli1 is involved in WNV replication in neural cells and induction of inflammatory cytokines and chemokines in human microglial cells.

To determine if defective replication contributes to attenuated inflammatory responses in the CNS, we infected WT microglial cells with WNV passaged in WT or *Peli1*$^{-/-}$ neurons or macrophages. WT microglia- infected with WNV grown in *Peli1*$^{-/-}$ cells had lower viral titers (Figure 7, A and B) and reduced mRNA levels of *Il6*, *Ccl2*, and *Ccl7*, but not *Tnfa* and *Cxcl10* (Figure 7, C -E**)** compared to cells infected with WNV grown in WT cells. It is known that microglia respond to viral infection via activation of p38MAPK (24). Microglia infected with WNV passaged in *Peli1*$^{-/-}$ cells also showed lower phosphorylation levels of p38MAPK than infected with WNV passaged in WT neurons (Figure 7F). Smaducin-6, a membrane-tethered palmitic acid-conjugated peptide composed of amino acids 422-441 of Smad6 was reported to interact with Peli1 and disrupt the formation of IRAK1, RIP-1, and IKKε, but not MAPK mediated signaling complexes (34). Smaducin-6 treatment did not block WNV infection nor induction of inflammatory cytokine/chemokine production in microglial cells or macrophages, though it decreased levels of type 1 IFNs in macrophages (Figure 7G-H & Supplemental Figure 7). Overall, our results suggest that Peli1 is required for WNV replication in the neural cells which promotes p38MAPK activation in microglia and induction of inflammatory immune responses in the CNS.

DISCUSSION

Peli1 has been reported to be an important mediator in activation of NF-κB or p38MAPK in TLR- dependent signaling pathways (2). In this study, we have provided evidence demonstrating that Peli1 facilitates WNV replication and mediates innate immunity in the periphery and CNS (Figure 8). In particular, we conclude that Peli1 is predominantly involved in CNS neuroinflammation during WNV infection based on the following facts: First, although Peli1 promotes WNV replication in myeloid cells (macrophages and DCs), it also positively regulates antiviral innate immune responses in these cells, which compromise its overall pathogenic effects in the periphery. Second, compared to myeloid cells, Peli1 expression is highly enriched in CNS resident cells and is even upregulated following WNV infection. Third, Peli1 facilitates WNV replication in microglia and neurons, especially in the latter which are the major cells infected during in vivo challenge. It also positively mediates NF-KB and /or p38MAPK activation in these cells, and boosts a robust inflammatory cytokine and chemokine production, which attracts more inflammatory cells infiltrated from the periphery and ultimately contributes to lethal WNV encephalitis. Thus, Peli1 synergistically promotes virus dissemination and inflammation in the CNS. Lastly, *Peli1*$^{-/-}$ mice displayed similar levels of resistance compared to WT mice following systemic and direct intracranial WNV infection. This further indicates that Peli1 promotes WNV- induced pathology primarily in the CNS.

WNV-induced CNS disease is partially caused by bystander damage from both the immune response induced in the CNS residential cells (17, 18) and by infiltrating inflammatory cells (19-23). *Peli1*$^{-/-}$ mouse brains had a significantly decreased number of infiltrating CD4^{+} T cells, activated microglia, and macrophages. Both CCL2 and CCL7 are involved in the monocytosis and monocyte accumulation in the brain (35), whereas CXCL10 helps to recruit the antigen specific T cells (36). Microglial cells are the major producers of inflammatory cytokines and chemokines in the CNS following WNV infection (25, 37). In vitro WNV infection in *Peli1*$^{-/-}$ or Peli1- depleted mouse and human microglia resulted in a lower viral load and induced an

288 impaired production of IL-6, CCL2, CCL7, and CXCL10. Neurons are the primary targets during
289 in vivo WNV replication in the CNS (18, 38). WNV passaged in *Peli1*$^{-/-}$ neurons induced
290 similarly lower levels of p38MAPK phosphorylation in WT microglia, and this was accompanied
291 by impaired chemokine CCL2 and CCL7, but not CXCL10 production in these cells. Collectively,
292 our results suggest that Peli1 mediates proinflammatory cytokine and chemokine production
293 predominantly via facilitating WNV replication in neural cells (microglia and neurons), which
294 ultimately leads to macrophages/monocytes and T cell infiltration into the CNS.
295 In line with findings in a previous report (37), we did not note significant induction of
296 inflammatory cytokine responses in human neurons following WNV infection. Interestingly, WNV
297 induced higher *Peli1* expression on mouse neurons than on microglia. WNV-infected *Peli1*$^{-/-}$
298 mouse neurons had reduced levels of NF-κB and p38MAPK activation accompanied by an
299 impaired production of inflammatory cytokines and chemokines. It was also noted that non-
300 infected *Peli1*$^{-/-}$ mouse neurons also had lower levels p38MAPK activation despite of normal
301 basal levels of cytokine production compared to WT controls (data not shown). Thus, it is likely
302 Peli1-positively regulates inflammatory cytokine and chemokine responses in WNV-infected
303 mouse neurons via activation of NF-κB. Peli1 is known to activate NF-KB signaling via
304 interaction with RIPK1. RIPK3, another RIPK family member was recently shown to mediate
305 neuronal chemokine induction and recruit T lymphocytes and inflammatory myeloid cells in the
306 CNS (39). Whether Peli1 interacts with RIPK3 and regulates inflammatory responses remains
307 to be investigated.
308 Smad6 and Smad7 are critical mediators for effective TGF-β1-mediated suppression of
309 IL-1R/TLR signaling, by simultaneous binding to discrete regions of Peli1 (40). Smaducin-6,
310 which is composed of amino acids 422-441 of Smad6, has been reported to disrupt the
311 formation of IRAK1-, RIP1-, and IKKε-, mediated TRIF signaling complexes, but not
312 phosphorylation of p38MAPK in macrophages (34). Smaducin6 did not inhibit WNV replication

313 in microglia or macrophages. Further, Smaducin-6 did not block the production of inflammatory
314 cytokines and chemokines in WNV-infected microglia and macrophages. These results support
315 a role of Peli1 in induction of inflammatory responses in both cell types during WNV infection via
316 promoting p38MAPK activation.

317 Consistent with the findings in myeloid and CNS resident cells, the production of type I
318 IFNs, inflammatory cytokines, and chemokines in the blood and CNS tissues were all impaired
319 in WNV-infected *Peli1*$^{-/-}$ mice. Our results suggest a role of Peli1 as a positive regulator of
320 innate immunity. There are conflicting reports on the role of Peli1 in induction of type I IFN
321 response during viral infection. For example, Xiao *et al*. found that Peli1 negatively regulates
322 IFN signaling in microglia and macrophages during vascular stomatitis virus infection in the CNS
323 (41). Another group has shown that Peli1 interacts with DEAF1 and positively regulates IFNβ
324 production following Sendai virus infection (42). While our results are in line with the latter, the
325 main difference between ours and the previous findings is that Peli1 positively mediates immune
326 induction predominantly via facilitating WNV entry and replication.

327 WNV life cycle includes attachment/entry, translation, RNA replication, and egress of
328 viral particles. Although the virus relies heavily on host proteins during its life cycle (43, 44), our
329 understanding of the molecular interactions of virus and mammalian host cells and their impacts
330 on viral pathogenesis is currently limited. Previous RNA interference screening of human genes
331 responsible for interaction with WNV proteins identified the Ub ligase CBLL1 as being critical for
332 WNV internalization during in vitro infection (45). Several host factors, including AXL and TIM1
333 have been shown to be involved in flavivirus replication from in vitro cell culture studies.
334 However, their roles remain to be confirmed in vivo (46-48). In this study, by using both in vivo
335 and in vitro models, we have identified Peli1 as a novel host factor required for WNV initial cell
336 attachment, and entry, a process which further promotes TLR-mediated inflammatory responses
337 in mouse and human neural cells. Interestingly, the size of the virions generated after
338 passaging WT WNV once in *Peli1*$^{-/-}$ cells was reduced significantly. No genetic changes were

noted in the passaged viruses (data not shown). However, the reduction of virion size is likely due to an altered protein composition or changes on the ratio of viral proteins in the virions during virus assembly (49). In particular, the smaller viral particles produced in *Peli1*$^{-/-}$ cells are consistent with the size of recombinant subviral particles assembled in the endoplasmic reticulum during flavivirus infection in mammalian cells reported previously (50). The subviral particles consist of the pre-membrane (PrM)-E structural proteins, retain functional properties and are transported from the endoplasmic reticulum through the secretory pathways to undergo cleavage maturation by the cellular protease furin. Mutation of the furin recognition site of PrM of tick-borne encephalitis virus resulted in secretion of the smaller subviral particles. Altogether, our data suggest that Peli1 is involved in WNV attachment, entry and assembly. The smaller virions generated *Peli1*$^{-/-}$ cells had reduced replication rates in WT cells and triggered attenuated inflammatory responses in these cells which contribute to a higher resistance in WT mice. These results further support our hypothesis that Peli1- mediates inflammatory responses and promotes WNV encephalitis via facilitating virus replication. Consistent with our findings in the murine model, we also demonstrate Peli1 expression is associated with WNV infection and inflammatory cell activation in acute post-mortem WNV encephalitis patient hippocampal tissues. Results from this study provide us with a better understanding of the mechanisms by which WNV induce lethal encephalitis. They will ultimately help to identify therapeutic targets for intervention, such as Peli1 as a new strategy for development of the inhibitors of virus replication to prevent and treat WNV-induced encephalitis. Lastly, Peli1 is expressed on many cell types and is highly enriched in the CNS tissues. Future investigation will be needed to determine the role of Peli1 in other virus models, in particular the neurotropic flaviviruses.

363 **METHODS**

364 **Mice:** 5-8-week-old C57BL/6 (B6) mice were purchased from the Jackson Laboratory.
365 *Peli1*$^{-/-}$ mice (on a B6 background) (2, 51) were bred at the University of Texas Medical Branch
366 (UTMB). Both female and male mice were used in this study and were age- and sex- matched.
367 Mice were inoculated intraperitoneally (i.p.) with100 FFU of WNV 385-99 (52, 53) or WNV 385-
368 99 passage once in WT and *Peli1*$^{-/-}$ macrophages. In some experiments, mice were challenged
369 intracranially (i.c.) with 5 FFU of WNV 385-99.

370 **Cells:** Bone marrow (BM)-derived dendritic cell (DC)s, macrophages, and primary
371 microglia cultures were isolated as described previously (2, 54). Neurons were generated
372 according to (55) with slight modifications. After the dissection and dissociation of cortices of
373 mouse embryos (E18.5), cells were enriched using a mouse neuron isolation kit (Miltenyi
374 Biotec) and cultured for 5 days in neurobasal medium containing B-27 supplement (Invitrogen).
375 BV2 cells were kindly provided by Dr. A Cardona (University of Texas San Antonio). BM-DCs or
376 macrophages, microglia, and BV2 cells were infected with WNV at a MOI of 0.1, or 0.02 and
377 neurons were infected at a MOI of 0.003. SH-SY5Y cells were cultured in F12K medium and
378 EMEM (Invitrogen) and seeded in the 6-well plate for 1 day, then replaced with fresh medium
379 with 30 uM Retinoic acid 1% (Sigma) and B27 Supplements (Gibco,17504) for 5 days, the cells
380 were differentiated to neurons. Smaducin-6 or Pal-Scram peptides (34) were purchased from
381 Sigma-Aldrich and used at 100 nm 1 h after infection. Supernatants and cells were harvested at
382 24 h and 96 h pi to measure viral load and cytokine production. In some experiments, WT and
383 *Peli1*$^{-/-}$ macrophages or neurons were infected with WNV 385-99. Culture supernatants were
384 then harvested at day 4 for virus titration by FFA. Equal titers of viruses from WT and *Peli1*$^{-/-}$
385 culture were subsequently used for in vivo and in vitro infection studies.

386 **FFA:** Vero cells were incubated with sample dilutions for 1 h. A semi-solid overlay
387 containing 0.8% methylcellulose (Sigma-Aldrich), 3% fetal bovine serum, 1% Penicillin-
388 Streptomycin, and 1% L-glutamine was added. At 48 h, the semisolid overlay was removed,

cells were washed, and fixed with 1:1 of acetone: methanol solution for at least 30 min at -20ºC. Cells were next subjected to immunohistochemical staining with a rabbit WNV polyclonal antibody (the World Reference Center for Emerging Viruses and Arboviruses (WRCEVA), T35502) followed by goat anti-rabbit HRP-conjugated IgG (KPL, 474-1516) for 1 h. Cells were next incubated with a peroxidase substrate (Vector Laboratories) until color developed. The number of foci was used to calculate viral titers.

qPCR: Samples were re-suspended in Trizol (Invitrogen) for RNA extraction. cDNA was synthesized by using a qScript cDNA synthesis kit (Bio-Rad). The sequences of the primer sets for WNV envelope (*Wnve*), *Peli1*, *Peli2*, *Peli3*, and cytokines cDNA and PCR reaction conditions were described previously (2, 25, 36, 53, 56). The assay was performed in the CFX96 real-time PCR system (Bio-Rad). Gene expression was calculated based on C_t values by using the formula $2^{-[C_t(\text{target gene})-C_t(GAPDH \text{ or } \beta\text{-actin})]}$ (53).

Viral attachment and entry assays: BM-macrophages were incubated with WNV (MOI of 3 or 10) at 4°C for 1 h, allowing the virus to attach to the cell surface. After 1 h incubation, infected cells were washed three times with cold PBS to remove unbound virions. Cell surface-associated viruses were removed by washing with cold alkaline-high-salt solution (1 M NaCl and 50 mM sodium bicarbonate, pH 9.5). After twice cold-PBS washes, the cells were harvested, and suspended in 3 ml DMEM medium containing 2% FBS. Total cells were collected by centrifugation at 1,000 × g for 5 min. The cell pellets were resuspended in Trizol for RNA extraction to measure viral titer by qPCR. Some cells were further incubated at 37°C to initiate viral entry. At 1.5 h and 5 h pi, the infected cells were stringently washed to remove free virus as well as cell surface-associated virus, and the intracellular viral RNA was quantified by qPCR.

Transmission electron microscopy (TEM): Cells were washed with ice cold PBS and incubated on ice for 15 min before exposure to WNV (MOI= 10) for 1 h. Cells were then rinsed with ice cold PBS, resuspended in pre-warmed media and incubated at 37°C. At 0 h, 5 min, and

10 h pi, cells were pelleted and fixed for at least 1 h in a mixture of 2.5% formaldehyde and 0.1% glutaraldehyde in 0.05 M cacodylate buffer (pH 7.3) to which 0.01% picric acid and 0.03% $CaCl_2$ were added (EM fixative). The pellets were washed in 0.1 M cacodylate buffer followed by post-fixation in 1% OsO4 in 0.1M cacodylate buffer for 1 h, washed and *en bloc* stained with 2% aqueous uranyl acetate for 20 min at 60°C. The pellets were next dehydrated in ethanol, processed through propylene oxide, and embedded in Poly/Bed 812 (Polysciences). Sections were cut on Leica EM UC7 ultramicrotome (Leica Microsystems), stained with lead citrate, and examined in a Philips CM-100 transmission electron microscope at 60 kV. Images were acquired with a Gatan Orius SC200 digital camera. In some experiments, supernatants of WNV-infected cells were concentrated at day 4 pi using a 3 kD spin columns (Sartoris, Germany). The concentrated supernatants were centrifuged for 10 min at 3000 xg to remove debris. Next, nickel grids were incubated with clarified supernatants for 10 min followed by glutaraldehyde fixation and 2% uranyl acetate staining. Micrographs were taken using a CM100 transmission electron microscope (Philips).

Flow cytometry: Brain leukocytes were isolated as described before (20) and were stained with antibodies for cell surface markers, including CD3 (eBioscience, clone 145-2C11), CD4 (eBioscience, clone GK1.5), CD8 (eBioscience, clone 53-6.7), CD11b (eBioscience, clone M1/70, Gr-1-(eBioscience, clone RB6-8C5) and CD45 (BD Biosciences, clone 30-F11), fixed with 1% paraformaldehyde in PBS and examined with a C6 Flow Cytometer (BD Biosciences). Dead cells were excluded on the basis of forward and side light scatter.

Western blot: Protein was dissolved in 1X SDS loading buffer, separated on SDS-PAGE gels, electroblotted onto nitrocellulose membranes, probed with primary and secondary antibodies, and detected using the enhanced chemiluminescence (ECL) system (Pierce). The primary antibodies against phospho-p38 (Thr180/Tyr182, #9211s), p38 (#9212), Phospho-NF-κB RelA (Ser 468, #3039) and NF-κB (#3034) were from Cell Signaling Technology (Beverly) and mouse monoclonal anti-β-actin (Sigma-Aldrich, clone AC-15) was used as a loading control.

Histology: Mice were transcardially perfused with PBS. Brains and spleens were removed and placed in 4% paraformaldehyde (PFA) for 3 days at 4°C, followed by 70% ethanol before embedding in optimal cutting temperature compound. H & E staining was performed at the Histopathology Laboratory Core at Baylor College of Medicine.

Immunohistochemistry: Human paraffin-embedded hippocampal tissues were obtained from fatal WNV encephalitis cases (generously provided by Dr. Beth Levy at St. Louis University, St. Louis, MO) and control post-mortem cases from patients without neurologic diseases (St. Louis, MO). Sections were deparaffinized in Xylene, rehydrated in serial dilutions of ethanol and boiled in citrate buffer (pH 6.0) for 30 min for antigen retrieval. Next, they were incubated for 2 h at room temperature in blocking solution (10% serum and .2% Tween 20 in PBS) to permeabilize and block nonspecific binding. This was followed by incubating with primary antibodies for Peli1 (Santa Cruz Biotechnology, sc-271065, 1:50), WNV antigen (UTMB WRCEVA, T35502, 1:500) and NeuN (Millipore, clone A60, 1:20) or isotype matched IgG in PBS supplemented with10%serum O/N at 4°C. After washing, sections were incubated for 1 h at room temperature with fluorescently conjugated secondary antibodies (Life Technologies, 1:500). Autofluorescence was darkened using .5% Sudan Black B (diluted in 70% Ethanol) incubated for 10 min. After washing, nuclei were counterstained with Dapi and coverslips were applied with ProLong™ Gold Antifade Mountant (ThermoFisher Scientific). Immunofluorescence was captured using a Zeiss LSM 510 laser-scanning confocal microscope.

Statistics: Survival curve comparisons were performed using Prism software (GraphPad) statistical analysis, which uses the log rank test. Values for viral burden, cytokine production, and antibody and T cell responses experiments were presented as means ± SEM. *P* values of these experiments were calculated with a non-paired 2-tailed Student's t test. Statistical significance was accepted at $P < 0.05$.

Study approval: All experiments were performed in compliance with and under the approval of the Animal Care and Use Committee at UTMB.

AUTHOR CONTRIBUTION

H.L., E.R.W., S.C., P.W., W.Z., S.J.T, P.V.A., and T.W. designed the experiments. E.R.W., H.L., E.M., J.A. S., W.R., L.L.V., S.Z., J.G., N.E.B., C.C., G.X., G.L., R.T., V.L.P., and T.W. performed the experiments. E.R.W., H.L., E.M., J.A.S., S.Z., B.H.P., C.C., V.L.P., W.Z., R.S.K., P.V.A., and T.W. analyzed the data. S.C., S.P.Y., W.Z., and S.C.S. provided key reagents. H.L., E.R.W., J.A.S., P.W., R.S.K., P.V.A. and T.W. wrote the manuscript.

ACKNOWLEDGEMENTS

This work was supported in part by the Institute for Human Infections & Immunity at UTMB (T.W.), NIH grants R01 AI099123 (T.W.), R01 AI27744 (T.W.), R01NS079166 (S.J.T), R01NS095747 (S.J.T), R01DA036165 (S.J.T), U19 AI083019 (R.S.K.) and R01 NS052632 (R.S.K.), and R01 EY022694 and R01 EY026629 (W.Z.). J.A.S was supported by NIH grant F31 AI124662-01. P.V.A and V.P were partially supported by NIH grant R24 AI120942. We thank Texas A&M Institute for Genomic Medicine for *Peli1*$^{-/-}$ mice, Dr. A Cardona from the University of Texas San Antonio and Dr. Partha Sarkar from UTMB for BV2 cells and SHSY-5Y cells, Dr. Beth Levy for human post-mortem hippocampal tissues, Ms. Lan Pang for technique support, and Dr. Linsey Yeager for assisting in manuscript preparation.

COMPETING FINANCIAL INTERESTS

The authors declare no competing financial interests.

REFERENCES:

1. Chang M, Jin W, and Sun SC. Peli1 facilitates TRIF-dependent Toll-like receptor signaling and proinflammatory cytokine production. *Nat Immunol.* 2009;10(10):1089-95.
2. Xiao Y, Jin J, Chang M, Chang JH, Hu H, Zhou X, et al. Peli1 promotes microglia-mediated CNS inflammation by regulating Traf3 degradation. *Nat Med.* 2013;19(5):595-602.
3. Chang M, Jin W, Chang JH, Xiao Y, Brittain GC, Yu J, et al. The ubiquitin ligase Peli1 negatively regulates T cell activation and prevents autoimmunity. *Nat Immunol.* 2011;12(10):1002-9.
4. Park HY, Go H, Song HR, Kim S, Ha GH, Jeon YK, et al. Pellino 1 promotes lymphomagenesis by deregulating BCL6 polyubiquitination. *The Journal of clinical investigation.* 2014;124(11):4976-88.
5. Laboratory-acquired West Nile virus infections--United States, 2002. *MMWR Morb Mortal Wkly Rep.* 2002;51(50):1133-5.
6. Charatan F. Organ transplants and blood transfusions may transmit West Nile virus. *Bmj.* 2002;325(7364):566.
7. Petersen LR, Brault AC, and Nasci RS. West Nile Virus: Review of the Literature. *JAMA.* 2013;310(3):308-15.
8. Carson PJ, Konewko P, Wold KS, Mariani P, Goli S, Bergloff P, et al. Long-term clinical and neuropsychological outcomes of West Nile virus infection. *Clin Infect Dis.* 2006;43(6):723-30.
9. Ou AC, and Ratard RC. One-year sequelae in patients with West Nile Virus encephalitis and meningitis in Louisiana. *J La State Med Soc.* 2005;157(1):42-6.
10. Cook RL, Xu X, Yablonsky EJ, Sakata N, Tripp JH, Hess R, et al. Demographic and clinical factors associated with persistent symptoms after West Nile virus infection. *Am J Trop Med Hyg.* 2010;83(5):1133-6.

11. Sadek JR, Pergam SA, Harrington JA, Echevarria LA, Davis LE, Goade D, et al. Persistent neuropsychological impairment associated with West Nile virus infection. *J Clin Exp Neuropsychol.* 2010;32(1):81-7.
12. Nolan MS, Podoll AS, Hause AM, Akers KM, Finkel KW, and Murray KO. Prevalence of chronic kidney disease and progression of disease over time among patients enrolled in the Houston West Nile virus cohort. *PLoS One.* 2012;7(7):e40374.
13. Patel H, Sander B, and Nelder MP. Long-term sequelae of West Nile virus-related illness: a systematic review. *The Lancet Infectious Diseases.*15(8):951-9.
14. Sejvar JJ. Clinical Manifestations and Outcomes of West Nile Virus Infection. *Viruses.* 2014;6(2):606-23.
15. Weatherhead JE, Miller VE, Garcia MN, Hasbun R, Salazar L, Dimachkie MM, et al. Long-Term Neurological Outcomes in West Nile Virus–Infected Patients: An Observational Study. *The American Journal of Tropical Medicine and Hygiene.* 2015;92(5):1006-12.
16. Anastasiadou A, Kakoulidis I, Butel D, Kehagia E, and Papa A. Follow-up study of Greek patients with West Nile virus neuroinvasive disease. *Int J Infect Dis.* 2013;17(7):e494-7.
17. Quick ED, Leser JS, Clarke P, and Tyler KL. Activation of intrinsic immune responses and microglial phagocytosis in an ex vivo spinal cord slice culture model of West Nile virus infection. *Journal of virology.* 2014;88(22):13005-14.
18. Shrestha B, Gottlieb D, and Diamond MS. Infection and injury of neurons by West Nile encephalitis virus. *J Virol.* 2003;77(24):13203-13.
19. Brehin AC, Mouries J, Frenkiel MP, Dadaglio G, Despres P, Lafon M, et al. Dynamics of immune cell recruitment during West Nile encephalitis and identification of a new CD19+B220-BST-2+ leukocyte population. *J Immunol.* 2008;180(10):6760-7.

20. Glass WG, Lim JK, Cholera R, Pletnev AG, Gao JL, and Murphy PM. Chemokine receptor CCR5 promotes leukocyte trafficking to the brain and survival in West Nile virus infection. *J Exp Med.* 2005;202(8):1087-98.

21. Lim JK, Obara CJ, Rivollier A, Pletnev AG, Kelsall BL, and Murphy PM. Chemokine receptor Ccr2 is critical for monocyte accumulation and survival in West Nile virus encephalitis. *J Immunol.* 2011;186(1):471-8.

22. Sitati E, McCandless EE, Klein RS, and Diamond MS. CD40-CD40 ligand interactions promote trafficking of CD8+ T cells into the brain and protection against West Nile virus encephalitis. *Journal of virology.* 2007;81(18):9801-11.

23. Sitati EM, and Diamond MS. CD4+ T-cell responses are required for clearance of West Nile virus from the central nervous system. *Journal of virology.* 2006;80(24):12060-9.

24. Town T, Jeng D, Alexopoulou L, Tan J, and Flavell RA. Microglia recognize double-stranded RNA via TLR3. *J Immunol.* 2006;176(6):3804-12.

25. Wang T, Town T, Alexopoulou L, Anderson JF, Fikrig E, and Flavell RA. Toll-like receptor 3 mediates West Nile virus entry into the brain causing lethal encephalitis. *Nat Med.* 2004;10(12):1366-73.

26. Vasek MJ, Garber C, Dorsey D, Durrant DM, Bollman B, Soung A, et al. A complement-microglial axis drives synapse loss during virus-induced memory impairment. *Nature.* 2016;534(7608):538-43.

27. Lazear HM, Lancaster A, Wilkins C, Suthar MS, Huang A, Vick SC, et al. IRF-3, IRF-5, and IRF-7 coordinately regulate the type I IFN response in myeloid dendritic cells downstream of MAVS signaling. *PLoS Pathog.* 2013;9(1):e1003118.

28. Mukhopadhyay S, Kim BS, Chipman PR, Rossmann MG, and Kuhn RJ. Structure of West Nile virus. *Science.* 2003;302(5643):248.

29. Fredericksen BL, and Gale M, Jr. West Nile virus evades activation of interferon regulatory factor 3 through RIG-I-dependent and -independent pathways without antagonizing host defense signaling. *Journal of virology.* 2006;80(6):2913-23.
30. Daffis S, Samuel MA, Suthar MS, Gale M, Jr., and Diamond MS. Toll-like receptor 3 has a protective role against West Nile virus infection. *Journal of virology.* 2008;82(21):10349-58.
31. Town T, Bai F, Wang T, Kaplan AT, Qian F, Montgomery RR, et al. Toll-like receptor 7 mitigates lethal West Nile encephalitis via interleukin 23-dependent immune cell infiltration and homing. *Immunity.* 2009;30(2):242-53.
32. Kelley TW, Prayson RA, Ruiz AI, Isada CM, and Gordon SM. The neuropathology of West Nile virus meningoencephalitis. A report of two cases and review of the literature. *Am J Clin Pathol.* 2003;119(5):749-53.
33. Cho H, Proll SC, Szretter KJ, Katze MG, Gale M, Jr., and Diamond MS. Differential innate immune response programs in neuronal subtypes determine susceptibility to infection in the brain by positive-stranded RNA viruses. *Nat Med.* 2013;19(4):458-64.
34. Lee YS, Park JS, Jung SM, Kim SD, Kim JH, Lee JY, et al. Inhibition of lethal inflammatory responses through the targeting of membrane-associated Toll-like receptor 4 signaling complexes with a Smad6-derived peptide. *EMBO Mol Med.* 2015;7(5):577-92.
35. Bardina SV, Michlmayr D, Hoffman KW, Obara CJ, Sum J, Charo IF, et al. Differential Roles of Chemokines CCL2 and CCL7 in Monocytosis and Leukocyte Migration during West Nile Virus Infection. *J Immunol.* 2015.
36. Klein RS, Lin E, Zhang B, Luster AD, Tollett J, Samuel MA, et al. Neuronal CXCL10 directs CD8+ T-cell recruitment and control of West Nile virus encephalitis. *J Virol.* 2005;79(17):11457-66.

37. Cheeran MC, Hu S, Sheng WS, Rashid A, Peterson PK, and Lokensgard JR. Differential responses of human brain cells to West Nile virus infection. *J Neurovirol.* 2005;11(6):512-24.

38. Sampson BA, Ambrosi C, Charlot A, Reiber K, Veress JF, and Armbrustmacher V. The pathology of human West Nile Virus infection. *Hum Pathol.* 2000;31(5):527-31.

39. Daniels BP, Snyder AG, Olsen TM, Orozco S, Oguin TH, 3rd, Tait SW, et al. RIPK3 Restricts Viral Pathogenesis via Cell Death-Independent Neuroinflammation. *Cell.* 2017;169(2):301-13 e11.

40. Lee YS, Kim JH, Kim ST, Kwon JY, Hong S, Kim SJ, et al. Smad7 and Smad6 bind to discrete regions of Pellino-1 via their MH2 domains to mediate TGF-beta1-induced negative regulation of IL-1R/TLR signaling. *Biochemical and biophysical research communications.* 2010;393(4):836-43.

41. Xiao Y, Jin J, Zou Q, Hu H, Cheng X, and Sun SC. Peli1 negatively regulates type I interferon induction and antiviral immunity in the CNS. *Cell Biosci.* 2015;5:34.

42. Ordureau A, Enesa K, Nanda S, Le Francois B, Peggie M, Prescott A, et al. DEAF1 is a Pellino1-interacting protein required for interferon production by Sendai virus and double-stranded RNA. *The Journal of biological chemistry.* 2013;288(34):24569-80.

43. Bidet K, and Garcia-Blanco MA. Flaviviral RNAs: weapons and targets in the war between virus and host. *Biochem J.* 2014;462(2):215-30.

44. Brinton MA. Replication cycle and molecular biology of the West Nile virus. *Viruses.* 2014;6(1):13-53.

45. Krishnan MN, Ng A, Sukumaran B, Gilfoy FD, Uchil PD, Sultana H, et al. RNA interference screen for human genes associated with West Nile virus infection. *Nature.* 2008;455(7210):242-5.

46. Govero J, Esakky P, Scheaffer SM, Fernandez E, Drury A, Platt DJ, et al. Zika virus infection damages the testes in mice. *Nature.* 2016;540(7633):438-42.

47. Miner JJ, Sene A, Richner JM, Smith AM, Santeford A, Ban N, et al. Zika Virus Infection in Mice Causes Panuveitis with Shedding of Virus in Tears. *Cell Rep.* 2016;16(12):3208-18.

48. Tabata T, Petitt M, Puerta-Guardo H, Michlmayr D, Wang C, Fang-Hoover J, et al. Zika Virus Targets Different Primary Human Placental Cells, Suggesting Two Routes for Vertical Transmission. *Cell host & microbe.* 2016;20(2):155-66.

49. Xu Z, and Hobman TC. The helicase activity of DDX56 is required for its role in assembly of infectious West Nile virus particles. *Virology.* 2012;433(1):226-35.

50. Allison SL, Tao YJ, O'Riordain G, Mandl CW, Harrison SC, and Heinz FX. Two distinct size classes of immature and mature subviral particles from tick-borne encephalitis virus. *Journal of virology.* 2003;77(21):11357-66.

51. Liu HM, Jiang F, Loo YM, Hsu S, Hsiang TY, Marcotrigiano J, et al. Regulation of Retinoic Acid Inducible Gene-I (RIG-I) Activation by the Histone Deacetylase 6. *EBioMedicine.* 2016;9:195-206.

52. Tesh RB, Siirin M, Guzman H, Travassos da Rosa AP, Wu X, Duan T, et al. Persistent West Nile virus infection in the golden hamster: studies on its mechanism and possible implications for other flavivirus infections. *J Infect Dis.* 2005;192(2):287-95.

53. Welte T, Aronson J, Gong B, Rachamallu A, Mendell N, Tesh R, et al. Vgamma4+ T cells regulate host immune response to West Nile virus infection. *FEMS Immunol Med Microbiol.* 2011;63(2):183-92.

54. Daffis S, Samuel MA, Suthar MS, Keller BC, Gale M, Jr., and Diamond MS. Interferon regulatory factor IRF-7 induces the antiviral alpha interferon response and protects against lethal West Nile virus infection. *Journal of virology.* 2008;82(17):8465-75.

55. Ru W, Peng Y, Zhong L, and Tang SJ. A role of the mammalian target of rapamycin (mTOR) in glutamate-induced down-regulation of tuberous sclerosis complex proteins 2 (TSC2). *Journal of molecular neuroscience : MN.* 2012;47(2):340-5.

56. Lanciotti RS, Kerst AJ, Nasci RS, Godsey MS, Mitchell CJ, Savage HM, et al. Rapid detection of West Nile virus from human clinical specimens, field- collected mosquitoes, and avian samples by a TaqMan reverse transcriptase-PCR assay. *J Clin Microbiol.* 2000;38(11):4066-71.

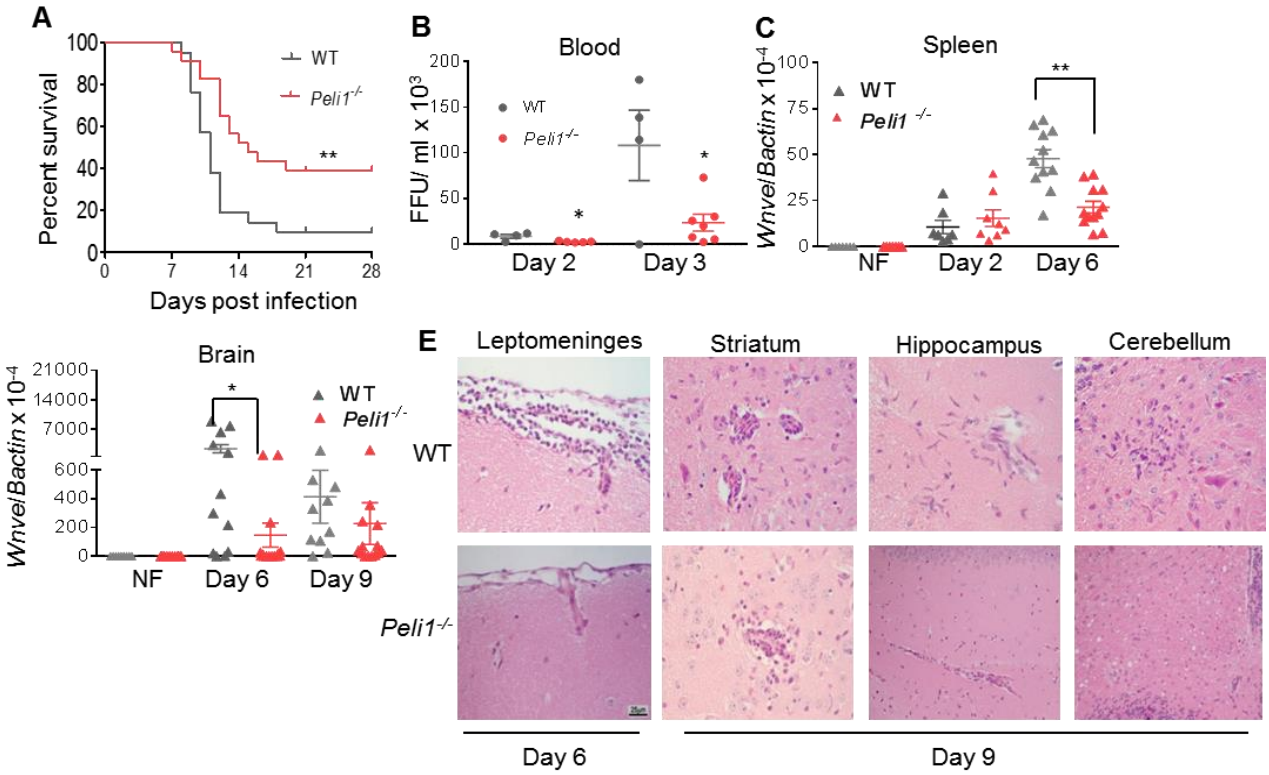

Figure 1. *Peli1*$^{-/-}$ mice are more resistant to lethal WNV infection. **A.** Survival of WT and *Peli1*$^{-/-}$ mice after i.p. injection with WNV 385-99. *n* = 21 and n = 23 for WT and *Peli1*$^{-/-}$ mice respectively. ** $P < 0.01$ compared to WT group (log rank test). **B.** Viremia was determined by using FFA at days 2 and 3 post infection (pi). Data are presented as mean ± SEM (n= 3 to 6) of samples collected from one representative of three similar experiments. **C-D.** Viral load in the spleen and brain of infected and non-infected (NF) mice was determined by qPCR assay. Data are presented as mean ± SEM, *n* = 7 to 12 collected from 3 independent experiments. For Panels **B-D**, ** $P < 0.01$ or *$P < 0.05$ compared to WT group (Unpaired t test). **E**. H &E staining. Representative images (20X) shown are brains collected from 4 to 5 WNV-infected mice per group at indicated time points. Scale bar: 100µm.

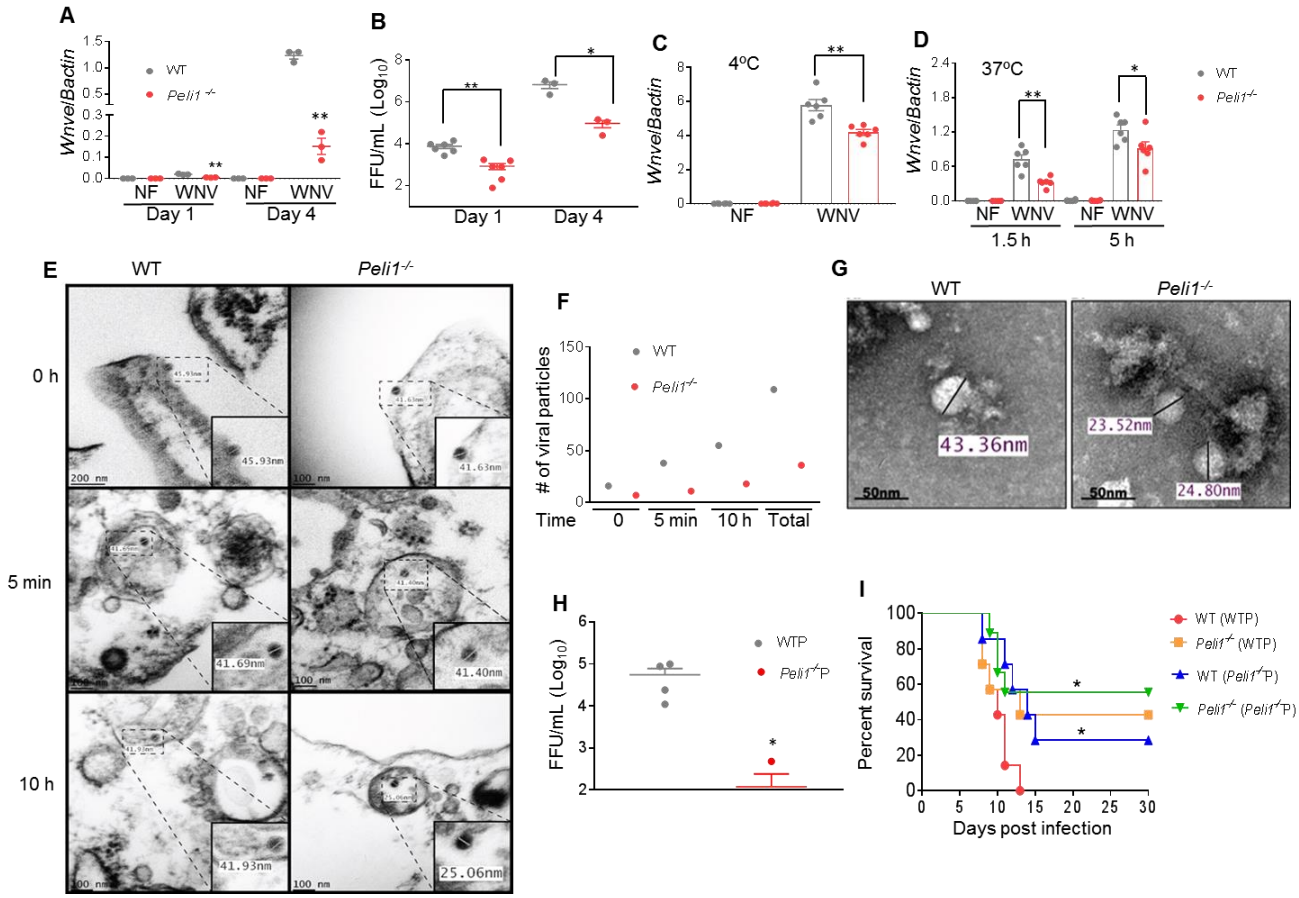

Figure 2. Peli1 facilitated WNV replication in macrophages and promoted high mortality in vivo. A-B. Viral load of WNV-infected macrophages was measured by qPCR (**A**) and FFA (**B**). Data shown are representative of five similar experiments and are presented as means ± SEM, *n* = 3 to 6. **C-D**. Macrophages were infected with WNV for 1 h at 4ºC, washed and collected to measure intracellular viral RNA by qPCR in the attachment assay (C). For virus entry (D), cells were subsequently resuspended in medium and incubated at 37ºC. At indicated time points, cells were washed to determine intracellular viral RNAs. n= 6. **E-F**. Thin-section transmission electron micrographs of WNV- infected macrophages. **E**. Viral particles were observed at the plasma membrane at 0 min, in small uncoated vesicles at 5 min and in double membrane vesicles at 10 h. **F**. Quantitation of 10 fields of view of ultrathin sections. **G.** Negative staining micrograph of WNV. Virions range in size from 41 nm to 47 nm and 23.5 nm to 39.5 nm in the supernatants of WT and *Peli1*$^{-/-}$ macrophages at day 4 pi respectively. **H**. WT macrophages were infected at MOI of 0.02 with viruses passaged in WT (WTP) and *Peli1*$^{-/-}$ (*Peli1*$^{-/-}$P) macrophages. Viral load was measured by FFA at day 4 pi. Data shown are representative of two similar experiments and are presented as means ± SEM, *n* = 4. Data in **A-D** & **H** were analyzed by Unpaired t test. ** *P* < 0.01 or **P* < 0.05 compared to WT group. **I.** Survival rate of mice i.p. injected with 100 FFU of WNV passaged in WT macrophages (WTP), and *Peli1*$^{-/-}$ (*Peli1*$^{-/-}$P) macrophages. *n*= 7 or 9. **P* < 0.05 compared to WT mice infected with WTP (WT (WTP), Log-rank test).

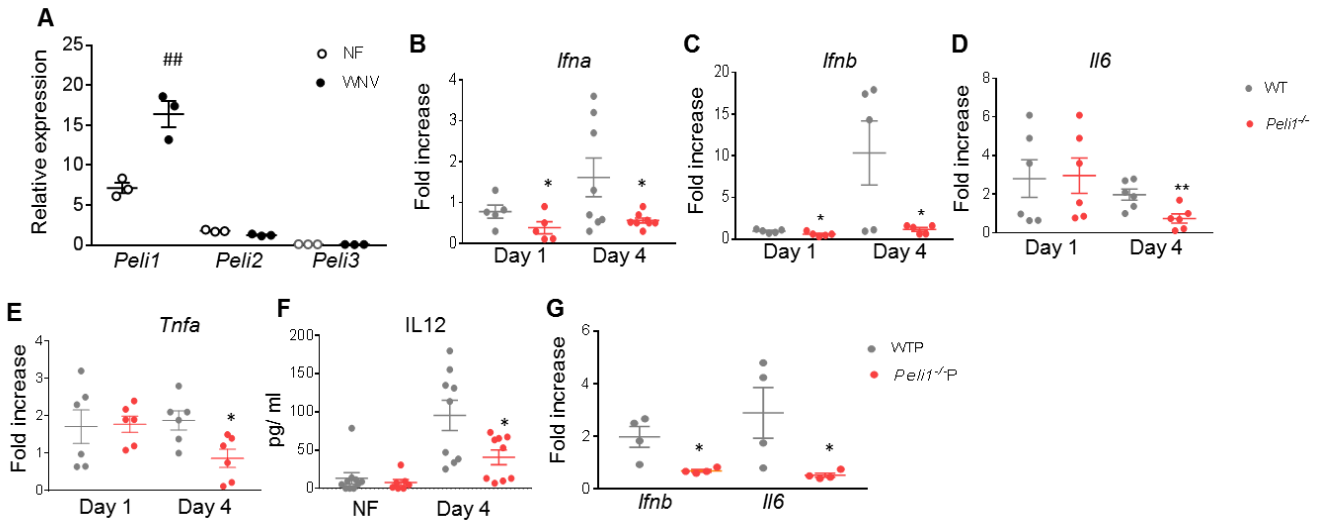

682

683
684

685 **Figure 3. WNV- induced antiviral immune responses in WT and *Peli1*$^{-/-}$ macrophages**. **A-**
686 **F.** WT and *Peli1*$^{-/-}$ macrophages were infected with WNV and harvested at indicated time
687 points. **A**. *Peli1*, *Peli2*, and *Peli3* RNA levels in WT macrophages were measured at day 4 pi.
688 Data shown are representative of three similar experiments and are presented as means ±
689 SEM, $n = 3$. $^{\#\#}$ $P < 0.01$ compared to non-infected (NF) group (Unpaired t test). **B- F.** Cytokine
690 RNA or protein levels were measured at indicated time points by qPCR and Bioplex
691 respectively. Data represent means ± SEM of 5 to 10 samples collected from 2 independent
692 experiments. ** $P < 0.01$ or *$P < 0.05$ compared to WT group. **G.** WT macrophages were
693 infected at MOI of 0.02 with WNV passaged in WT (WTP) or *Peli1*$^{-/-}$ (*Peli1*$^{-/-}$P) macrophages.
694 At day 4 pi, cytokine production was determined by using qPCR. Data are presented as the fold
695 increase compared to mock- infected (means ± SEM) and are representative of two similar
696 experiments, $n = 3$ to 6 per group. *$P < 0.05$ compared to WTP group (Unpaired t test).

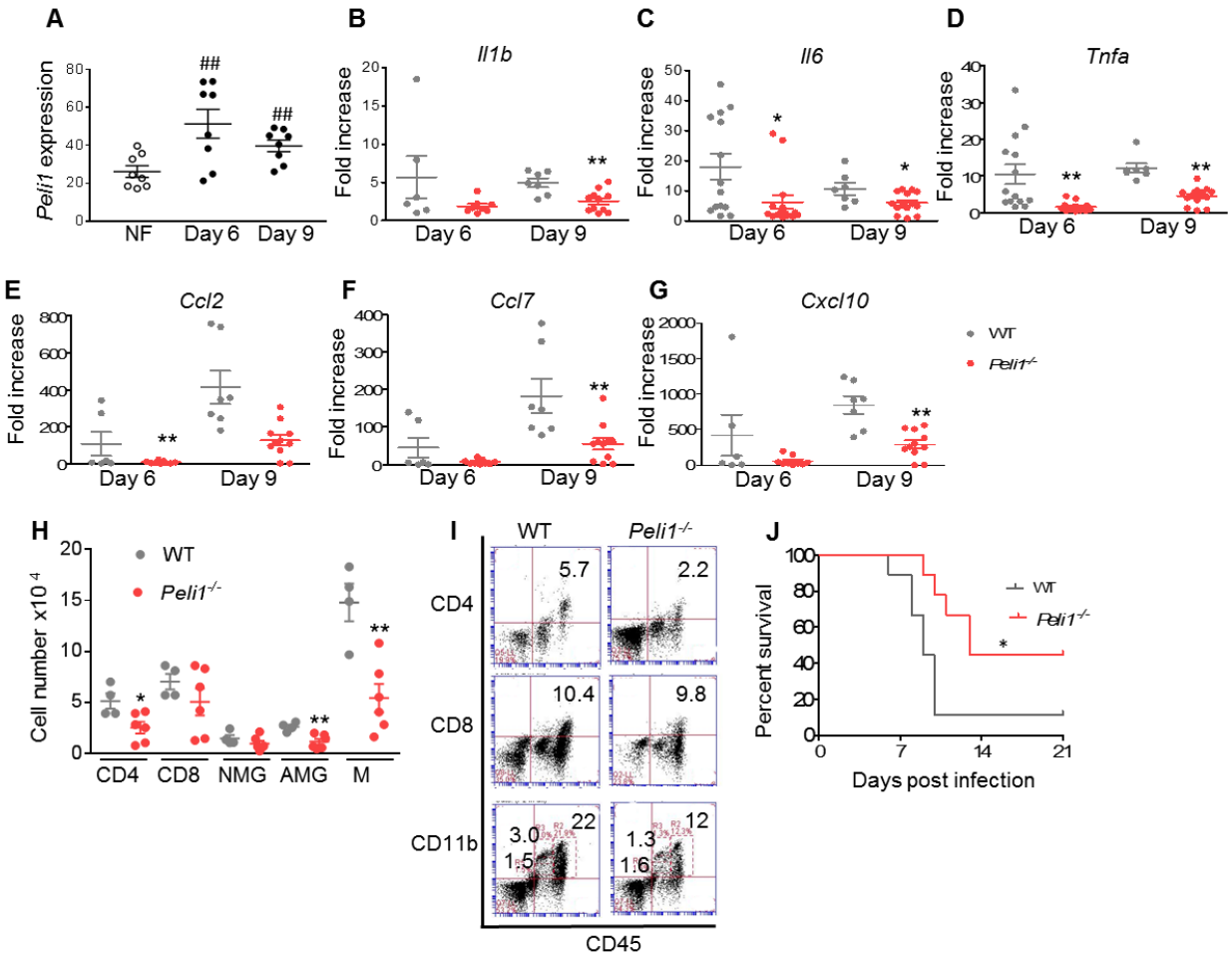

Figure 4. *Peli1* mediated neuroinflammation in the CNS after WNV infection. A. RNA levels of *Peli1* in the brain of WT mice following WNV infection were determined by qPCR assay. Data are presented as the means ± SEM of samples pooled from 2 to 3 independent experiments, n= 8. $^{\#\#}$ $P < 0.01$ compared to non-infected (NF) group (Unpaired t test). **B-G.** RNA levels of cytokines and chemokines in the brain at indicated time points were determined by qPCR assay. Data are presented as the means ± SEM of pooled 6 to 10 samples from 2 independent experiments. **H-J**. Brain leukocyte infiltration following WNV infection. **H.** The number of brain leukocytes are presented as the means ± SEM of 9 to 10 mice from 2 independent experiments, including naïve microglia cells (NMG), activated microglial cells (AMG), macrophages (M), $CD4^+$ and $CD8^+$ T cells on day 9 pi analyzed by flow cytometry. **I.** Representative flow image is shown. For **B-G** & H, ** $P < 0.01$ or *$P < 0.05$ compared to WT group (Unpaired t test). **J.** Survival of WT and *Peli1*$^{-/-}$ mice after i.c. injection with WNV 385-99. $n = 9$ per group. *$P < 0.05$ compared to WT group (Log-rank test).

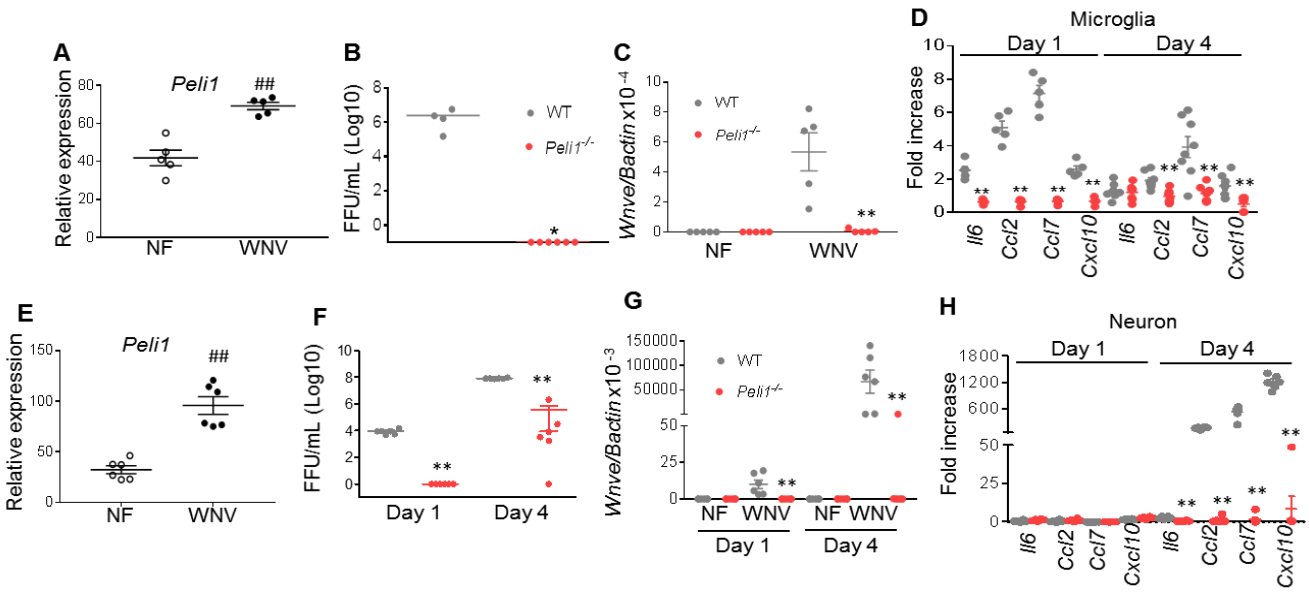

715
716
717 **Figure 5. WNV infection and induction of immune responses in microglia and neurons**.
718 **A.** RNA levels of *Peli1* in WT microglia at day 4 pi were determined by qPCR assay Data are
719 presented as means ± SEM and are representative of 2 independent experiments, n =5. ## $P <$
720 0.01 compared to non-infected (NF) group (Unpaired t test). **B- D.** Primary microglia were
721 infected with WNV 385-99 and harvested at indicated time points. Data are presented as the
722 means ± SEM of pooled 4 to 8 samples from 2 independent experiments. **B-C.** Viral load was
723 measured at day 4. **D.** Cytokine RNA levels were measured at indicated time points by qPCR.
724 **E- H**. Primary mouse neurons were infected with WNV 385-99 and harvested at indicated time
725 points. Data are presented as means ± SEM, n =6 per group. **E.** RNA levels of *Peli1* in WT
726 neurons at day 4 pi. ## $P < 0.01$ compared to NF group (Unpaired t test). **F-G**. Viral load was
727 measured at indicated time points by qPCR (**F**) and FFA (**G**). **H**. *Il6, Ccl2, Ccl7*, and *Cxcl10*
728 RNA levels were measured at indicated time points by qPCR. For **B-D & F-H** panels ** $P < 0.01$
729 or *$P < 0.05$ compared to WT group (Unpaired t test).

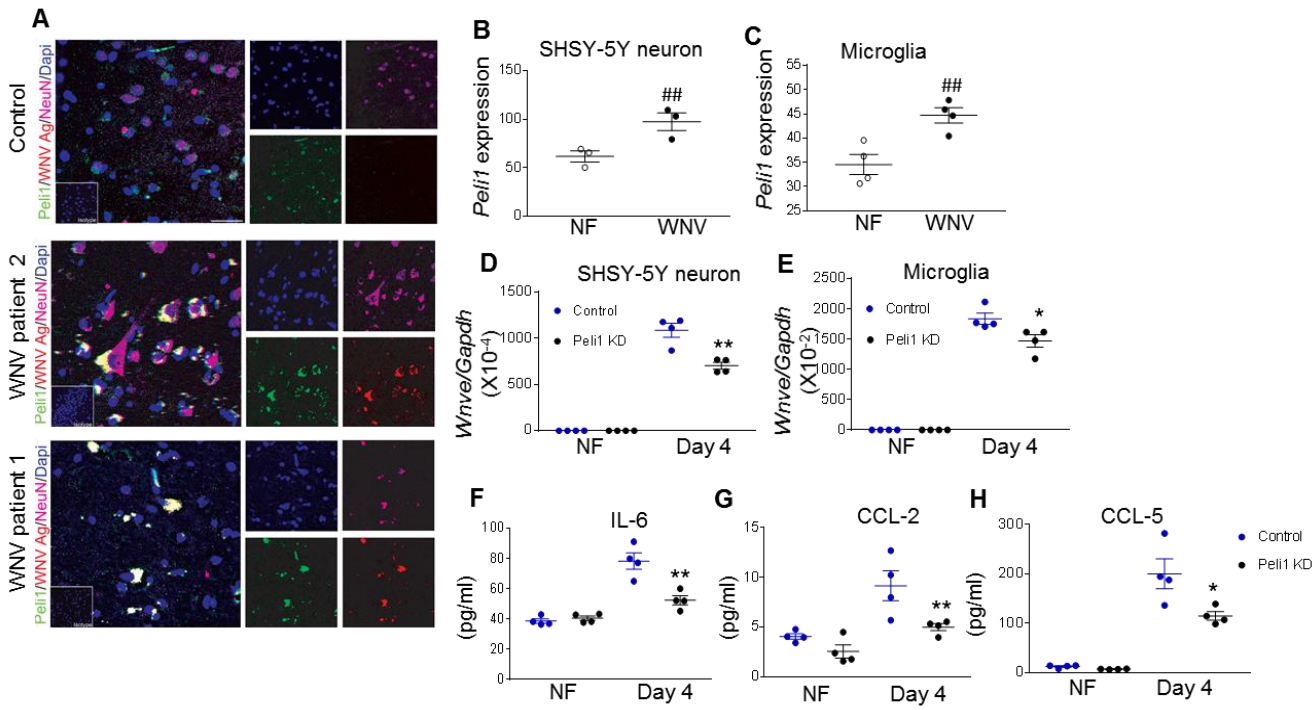

Figure 6. Peli1 expression and its role in human cells during WNV infection. A. Immunodetection of Peli1 (green), WNV antigen (red), and NeuN (purple), in postmortem hippocampal tissues from one control (top panel) or two WNV-infected patients (middle & bottom panels). Nuclei are counterstained with DAPI (blue). Scale bar: 8 µm. Insets: images of sections stained with isotype control antibodies or serum. **B- C.** RNA levels of *Peli1* in SH-SY5Y-derived neurons and human microglia at days 1 or 4 pi were determined by qPCR assay. Data are presented as means ± SEM and are representative of 2 similar experiments, n =3 to 4. ## $P < 0.01$ compared to NF group (Unpaired t test). **D- H.** SH-SY5Y- derived neurons (**D)** or human microglial cells (**E-H***)* were treated with control and Peli1 siRNA (Peli1KD), infected with WNV 385-99 at 48 h and harvested at indicated time points. **D- E**. Viral load was measured at day 4 by qPCR. **F- H**. IL-6, CCL-2, and CCL-5 production in microglial cells was measured at day 4 by Bioplex. Data are presented as means ± SEM and are representative of 2 similar experiments, n =4. ** $P < 0.01$ or *$P < 0.05$ compared to control group (Unpaired t test).

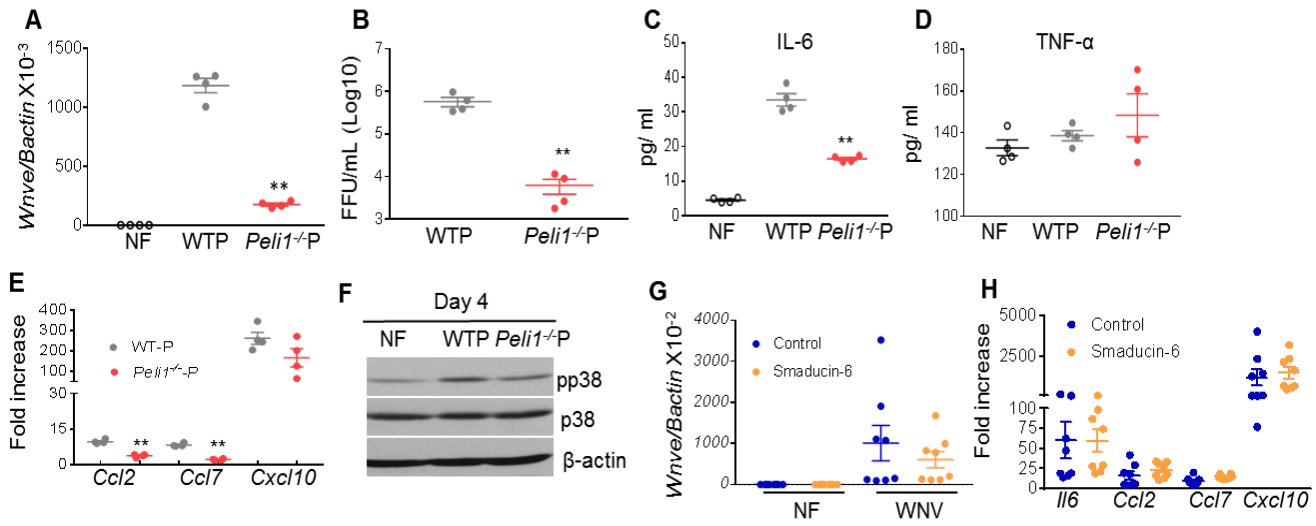

Figure 7. Peli1 promoted p38MAPK activation in microglia via facilitating WNV replication. **A- F.** BV2 cells were infected at MOI of 0.02 with viruses passaged in WT (WTP) and *Peli1*$^{-/-}$ (*Peli1*$^{-/-}$P) macrophages or neurons. **A- B.** At day 4 pi, viral load was measured by qPCR **(A)** or FFA (**B**). **C- E.** IL-6 and TNF-α production and *Ccl2*, *Ccl7*, and *Cxcl10* RNA levels were measured at day 4 by Bioplex or qPCR respectively. Data are presented as means ± SEM and are representative of 2 similar experiments, n =4. **A-E**, ** $P < 0.01$ compared to WT group (Unpaired t test). **F**. Western blot assay for p38MAPK activation. One representative of two samples per group was shown. **G**-**H**. BV2 cells were infected at MOI of 0.02 with WNV 385-99 and treated with Smaducin-6 or control peptides at 1 h pi. **G.** Viral load was measured at day 4 pi by qPCR. **H.** Cytokine and chemokine levels were measured at day 4 by qPCR. Data are presented as fold increase compared to mock- infected (means ± SEM) and represent 8 samples pooled from 2 independent experiments.

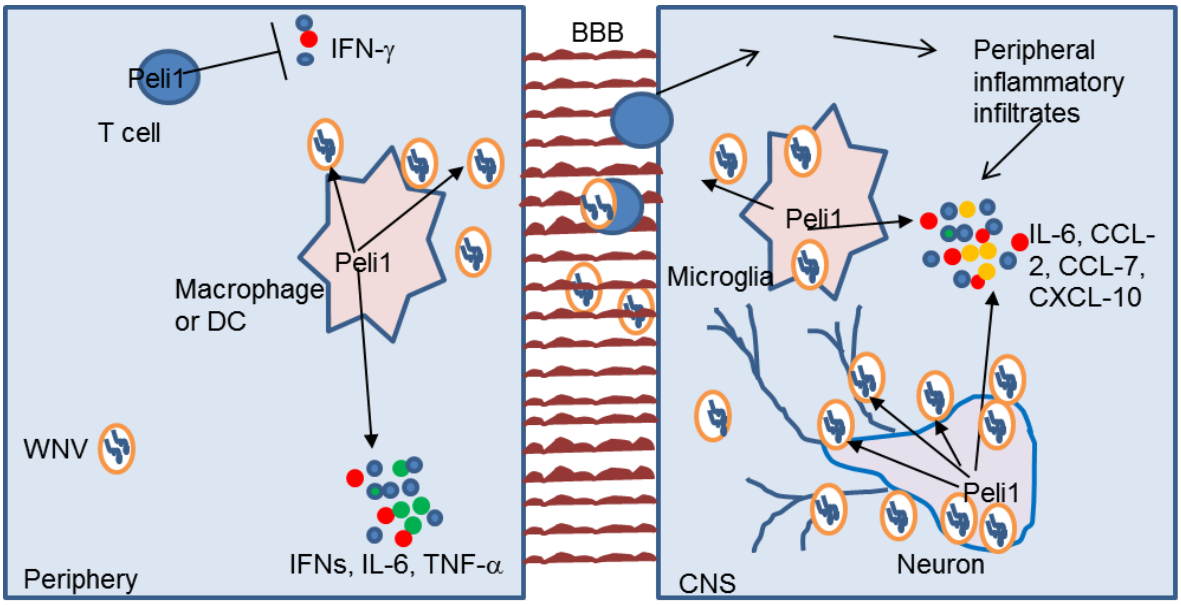

Figure 8. Proposed model illustrating Peli1 promotes virus replication and neuroinflammation during WNV infection.

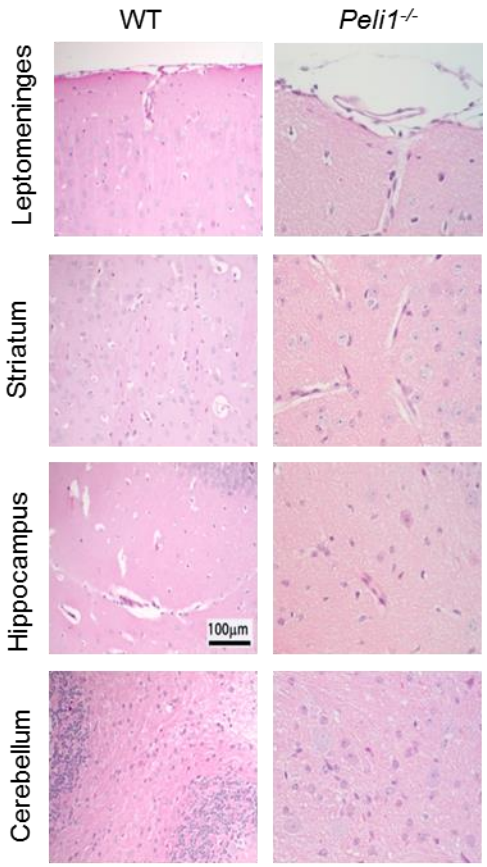

Supplemental Figure 1. **Histology study of WT and *Peli1*$^{-/-}$ mice.** Representative images (20X) shown are H&E staining of brains from non-infected WT and *Peli1*$^{-/-}$ mice. Samples were collected from 4 mice per group of 2 independent experiments. Scale bar: 100μm.

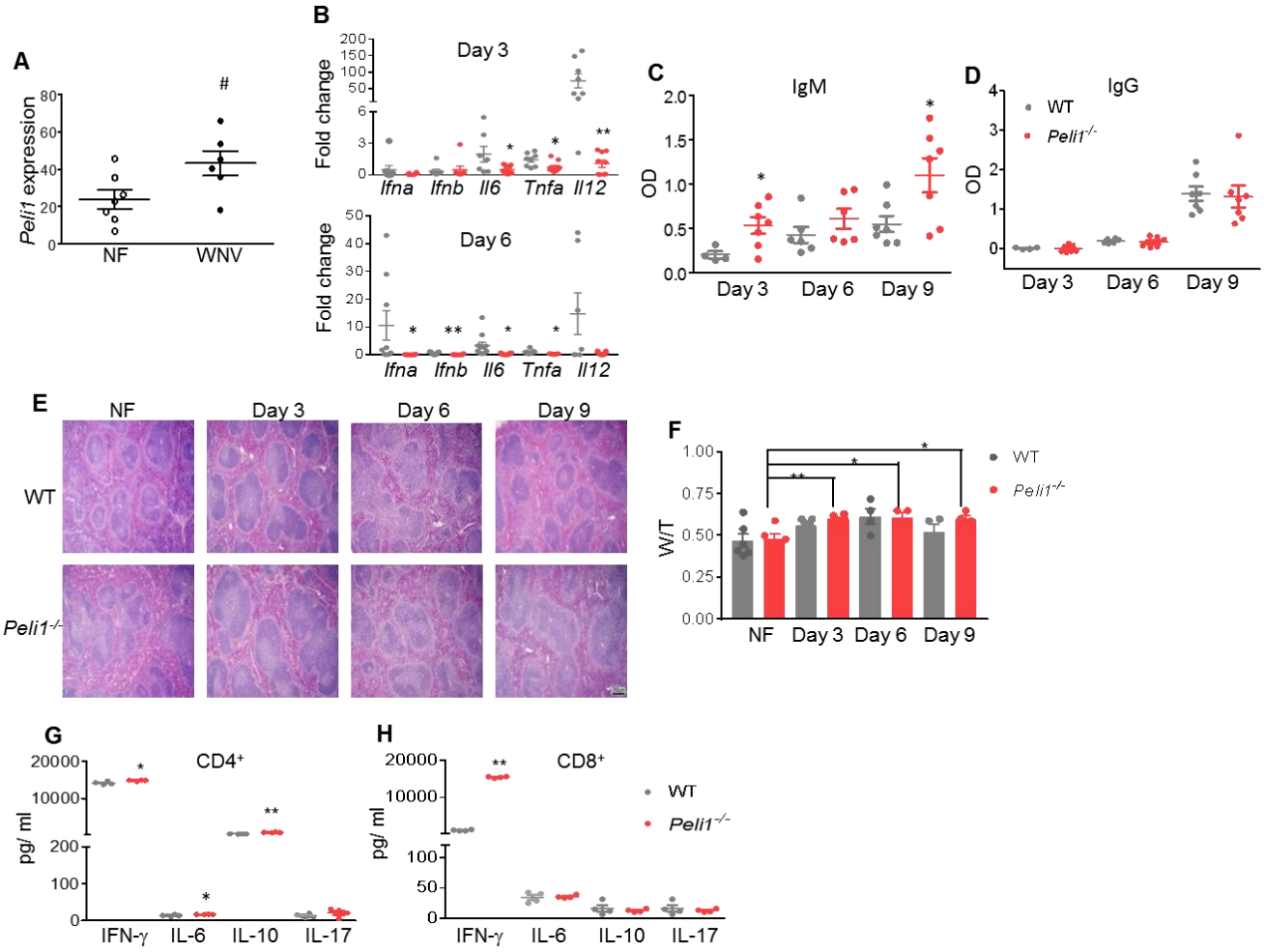

Supplemental Figure 2. *Peli1*$^{-/-}$ mice exhibited impaired cytokine production but modestly enhanced adaptive immune responses in the periphery. A. RNA levels of *Peli1* in the blood of WT mice at day 3 were determined by qPCR assay. Data represent the means ± SEM of 6 to 7 samples from 2 independent experiments. $^{\#}$ $P < 0.05$ compared to non-infected (NF) group (Unpaired t test). **B.** Blood cytokines levels were determined by qPCR assay. Data are presented as the fold increase compared to NF group and represent the means ± SEM of 6 to 11 samples from 3 independent experiments. **C- D**. The development of specific IgM (C) or IgG (D) Abs to WNV was determined using purified rWNV-E protein antigen. Data represent the means ± SEM of 4 to 7 samples from 2 independent experiments. **E-F*:*** H&E staining. Representative images (20X) shown are spleens from NF and WNV-infected mice. Two photographs of different regions were taken from each spleen section at lowest magnification (2.5X objective) to cover maximal area for comparison. The white pulp area was measured, expressed in pixels, using the ImageJ program (https://imagej.nih.gov/ij/). Scale bar: 250µm. Data are presented as the ratios of white pulp-to-total area (W/T) of each group and represent the means ± SEM, n= 2 to 3. ** $P < 0.01$ or *$P < 0.05$ compared to NF group (Unpaired t test). **G- H**. Splenocytes were harvested at day 7 pi and were cultured ex vivo with WNV peptides for 3 days, and cytokine production in culture supernatant was measured. Data represent the means ± SEM of 4 to 7 samples from 2 independent experiments. For **B-D & G-H** panels, ** P < 0.01 or *P < 0.05 compared to WT group (Unpaired t test).

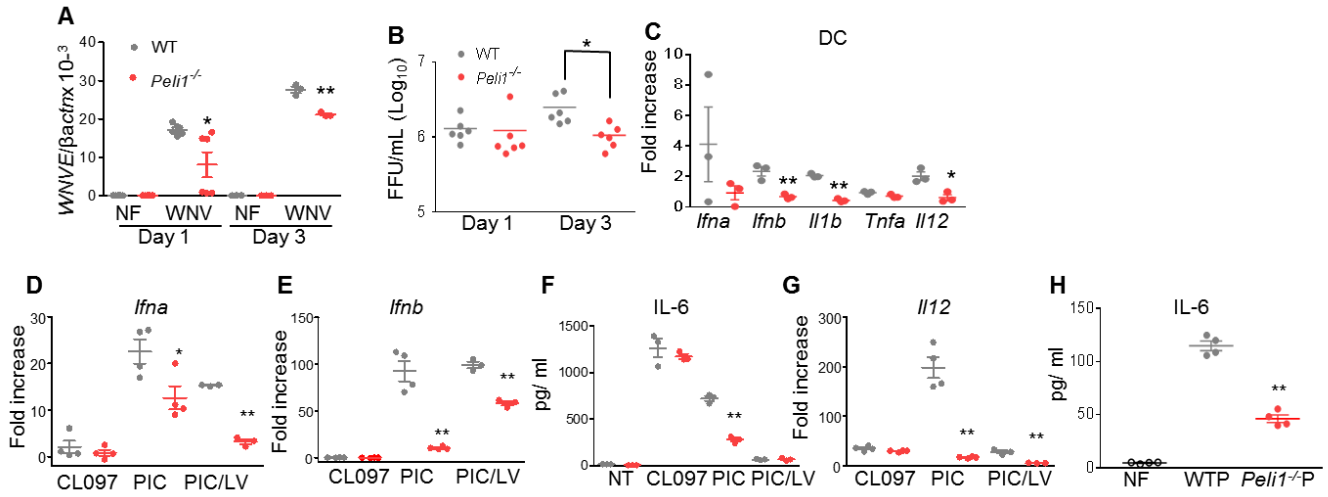

Supplemental Figure 3. WNV infection and PRR agonist treatment in *Peli1*$^{-/-}$ DCs and macrophages. A-C. WT and *Peli1*$^{-/-}$ DCs were infected with WNV. Viral load was measured at indicated time points by qPCR (**A**) and FFA (**B**). **C**. Cytokine RNA levels were measured at day 3. Data represent the means ± SEM of 3 to 6 samples from 2 independent experiments. **D- G**. WT and *Peli1*$^{-/-}$ macrophages were treated with TLR3, TLR7, and RLR agonists for 24 h. *Ifna*, *Ifnb*, *Il12* RNA and IL-6 protein levels were measured by qPCR or Bioplex. Data are presented as fold increase compared to NF or mock-treated cells. Data represent the means ± SEM of 3 to 4 samples are representative of 2 independent experiments. **A-G**, ** P < 0.01 or *P < 0.05 compared to WT group (Unpaired t test). **H.** WT macrophages were infected at MOI of 0.02 with WNV passaged in WT (WTP) or *Peli1*$^{-/-}$ (*Peli1*$^{-/-}$P) macrophages. At day 4 pi, IL-6 production was determined by Bioplex. Data represent the means ± SEM of 4 samples from 2 independent experiments. ** P < 0.01 compared to WTP group (Unpaired t test).

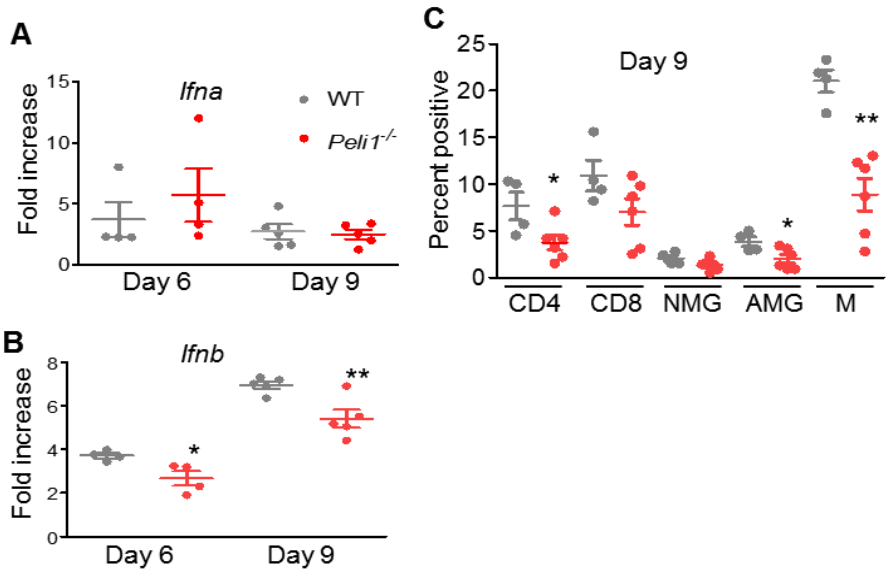

Supplemental Figure 4. **Type I IFN induction and leukocyte infiltration in the CNS. A-B**. RNA levels of type I IFNs in the brain at indicated time points were determined by qPCR assay. Data are presented as fold increase compared to NF group *(*means ± SEM) and represent 4 to 5 samples pooled from 2 independent experiments. **C**. Brain leukocyte infiltration following WNV 385-99 infection. The percentage (means ± SEM) of brain leukocytes collected from 9 to 10 mice of 2 independent experiments, including naïve microglia cells (NMG), activated microglial cells (AMG), macrophages (M), $CD4^+$ and $CD8^+$ T cells on day 9 pi was analyzed by flow cytometry. ** $P < 0.01$ or *$P < 0.05$ compared to WT group (Unpaired t test).

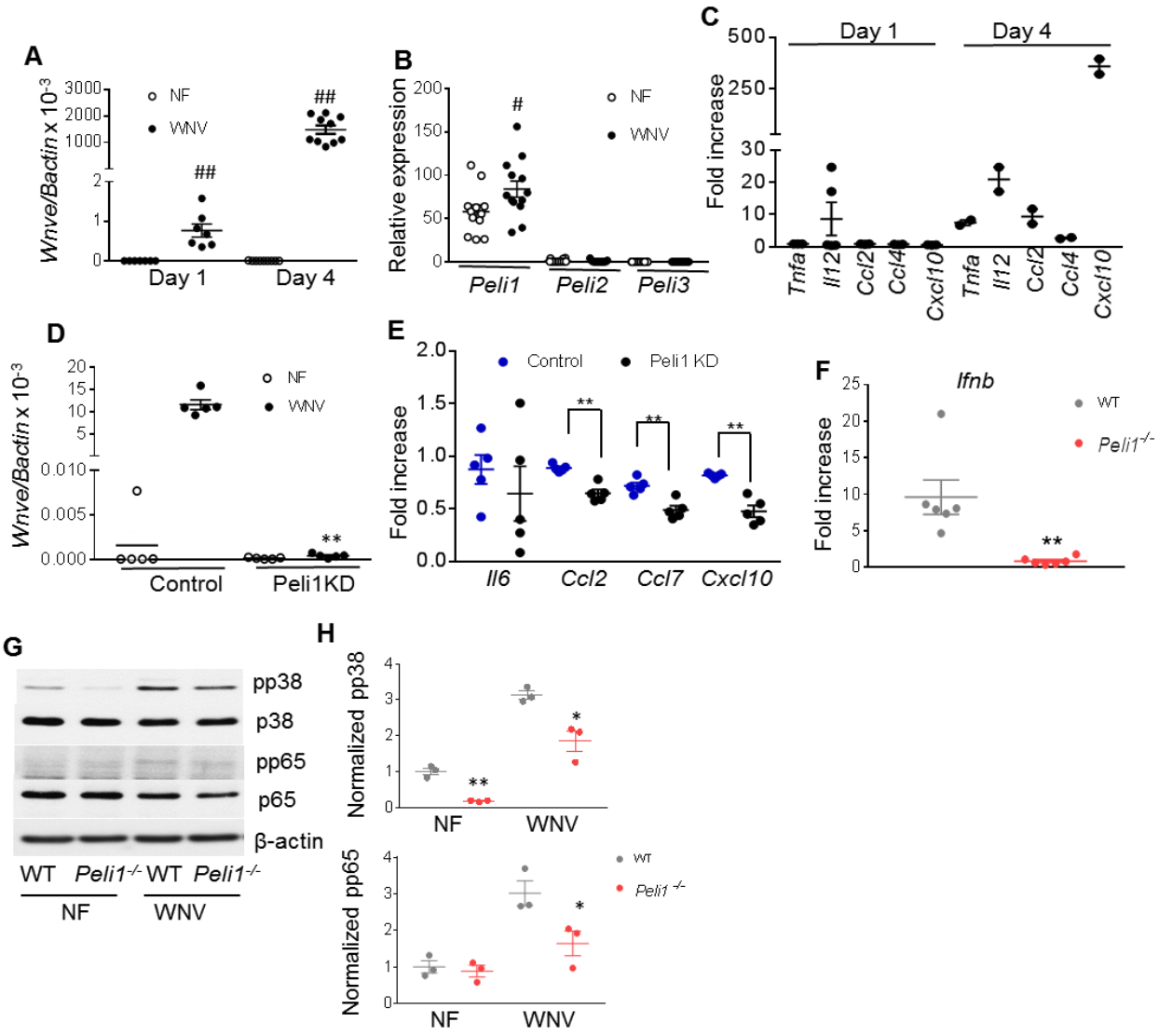

Supplemental Figure 5. **WNV infection in microglia and neurons. A- C**. BV2 cells were infected with WNV 385-99. **A.** Viral load was measured at indicated time points by qPCR. Data represent the means ± SEM of 7 to 10 samples pooled from 2 independent experiments. **B.** *Peli1*, *Peli2* and *Peli3* RNA levels in BV2 cells were measured by qPCR at day 4 pi. Data represent the means ± SEM of 12 to 13 samples pooled from 3 independent experiments. **A-B**, $^{\#\#}P < 0.01$ or $^{\#}P < 0.05$ compared to non-infected (NF) group (Unpaired t test). **C.** RNA levels of cytokines were measured at indicated time points. Data are presented as means ± SEM and are representative of 2 independent experiments (n = 2 to 3). **D- E.** BV2 cells were treated with control and Peli1 siRNA (Peli1KD) and infected with WNV 385-99 at 24 h. Data are presented as means ± SEM and are representative of 2 independent experiments (n = 5). ** $P < 0.01$ compared to control group (Unpaired t test). **D.** Viral load was measured at day 4 by qPCR. **E.** *Il6, Ccl2, Ccl7, and Cxl10* RNA levels were measured at day 4. **F.** *Ifnb* RNA levels in mouse neurons at day 4 pi. Data are presented as means ± SEM, n =6 per group. **G-H**. Western blot assay for p38MAPK and NF-κB activation in NF and WNV-infected neurons at day 3 pi. **G.** One representative of three samples per group was shown. **H.** The densitometric analysis of western blot data. Data presented as the ratio of pP65 or pP38 to β-actin compared to NF control. For **F& H** panels, ** $P < 0.01$ or *$P < 0.05$ compared to WT group (Unpaired t test).

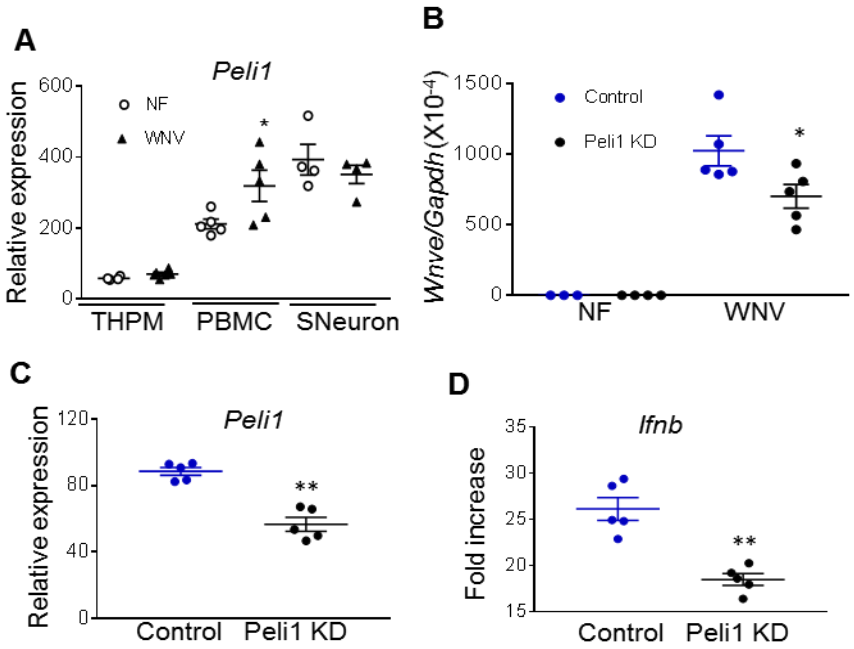

Supplemental Figure 6. **WNV infection in human cells**. **A.** RNA levels of *Peli1* in non-infected (NF) and WNV-infected hNSCs-derived neuron (SNeuron)s, THP1-derived macrophages (THPM) and peripheral blood mononuclear cell (PBMC)s were determined by qPCR assay. Data represent the means ± SEM of 4 to 6 samples pooled from 2 independent experiments. $^{\#}P < 0.05$ compared to non-infected (NF) group (Unpaired t test). **B- D**. S-neurons were treated with control and Peli1 siRNA knockdown (Peli1KD), infected with WNV 385-99 at 48 h and harvested at day 4 pi. Viral load (**B**) and *Ifnb* (**D**) levels were measured by qPCR. **C.** *Peli1* expression on control and Peli1 siRNA knockdown cells at 24 h post-treatment. Data represent the means ± SEM and are representative from 2 independent experiments, n =4 to 5. ** $P < 0.01$ compared to control group (Unpaired t test).

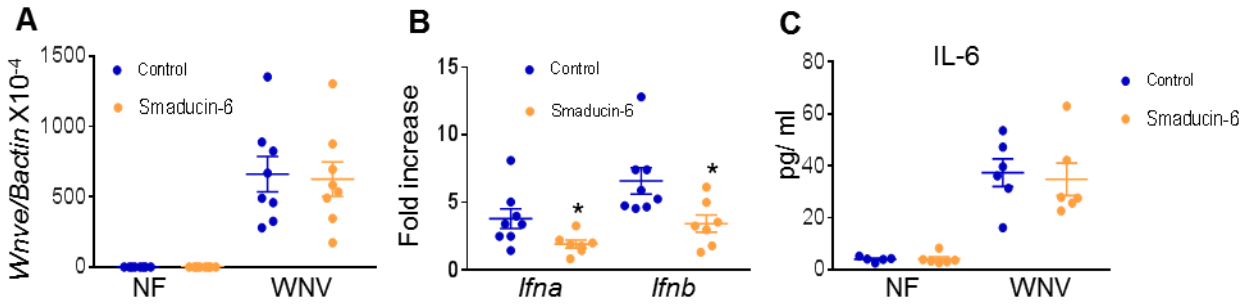

Supplemental Figure 7. **Smaducin-6 treatment in macrophages during WNV infection.** BM-macrophages were infected at MOI of 0.02 with WNV 385-99 and treated with Smaducin-6 or control peptides at 1 h pi. **A.** Viral load was measured at day 4 pi by qPCR. **B-C**. Cytokine levels were measured at day 4 by qPCR or Bioplex. Data are presented as fold increase compared to mock- infected or pg/ ml and represent the means ± SEM of 8 samples pooled from 2 independent experiments. *$P < 0.05$ compared to control group (Unpaired t test).

Table S1: Serum cytokine levels at day 3 post infection

Cytokine (pg/ml)	WT	*Peli1*$^{-/-}$
IL-1β	214.3 ± 5.2	184.1 ± 9.6*
IL-17	78.2 ± 10.5	87.2 ± 24.5
IFN-γ	22.3 ± 4.2	29.2 ± 2
IL-10	116.8 ± 10.5	70.6 ± 15.2*

Blood was harvested from WNV-infected mice at indicated time point post infection. Serum cytokine was measured by Bioplex. Data represent the means ± SEM and are representative of 2 independent experiments, n =4 per group. * $P < 0.05$ compared to WT group (Unpaired t test).

Supplemental Methods:

WNV infection in human cells: HMC3 (human microglial cell line), THP-1 cells and PBMCs from healthy donors were purchased from ATCC and Astarte Biologics, Inc respectively. THP-1 cells were treated with phorbol 12-myristate 13-acetate (PMA, Sigma) to differentiate into macrophage cells as described previously (57) before infection with WNV at a MOI of 1. HMC3 cells and PBMC were infected with WNV at a MOI of 5 or 10 respectively. Human fetal cortical neural stem cells (hNSCs) were propagated as neurospheres in DMEM/F12 basic media supplemented with 20 ng/mL epidermal growth factor (EGF), 20 ng/mL fibroblast growth factor 2 (FGF2), 10 ng/mL leukemia inhibitor factor (LIF) and N2; and passaged every 10 days (58). For neuron differentiation, dissociated hNSCs were plated into T75 flasks. After a 3-day incubation, 1.2×10^6 or 5×10^5 hNSCs (small spheres) were seeded into T25 flasks or 6-well plates pre-coated with 0.01% poly-D-lysine and 1 μg/cm^2 laminin (Invitrogen), respectively. Cells were incubated for 4 days with the priming media containing EGF (20 ng/mL), LIF (10 ng/mL) and laminin (1 μg/mL), followed by 9-day incubation with a differentiation medium consisting of N2 plus glutathione (1 μg/mL) (Sigma), biotin (0.1 μg/mL) (Sigma), superoxide dismutase (2.5μg/mL) (Worthington), DL-α-tocopherol (1 μg/mL, Sigma), DL--α-tocopherol acetate (1μg/mL, Sigma) and catalase (Sigma). Cells were subsequently infected with WNV at a MOI of 1.

In vitro T cell activation: Splenocytes (0.3×10^6) were stimulated with WNV-specific NS3 and E peptides respectively (59) for CD4$^+$ T cells, or WNV-specific NS4B and E peptides (60, 61) for CD8$^+$ T cells for 72 h at 37°C. Culture supernatant was collected for cytokine assay.

ELISA*:* Microtiter plates were coated with recombinant WNV-E protein (62) overnight at 4°C. Sera were diluted 1/30 in PBS with 2% BSA, and incubated for 1 h at room temperature. Alkaline phosphatase-conjugated goat anti-mouse IgG (Sigma-Aldrich, A3562) or IgM (Sigma-Aldrich, A9688) at a dilution of 1/1000 in 1XPBS with 0.05% Tween (Sigma-Aldrich) was then

added for 1 h. Color was developed with *p*-nitrophenyl phosphate (Sigma-Aldrich) and intensity read at an absorbance of 405 nm.

siRNA knockdown for Peli1: Mouse cells were transfected with 187.5nM of pooled Peli1 specific siRNA (CUCAUGACAGCAACACUGA, CAACCAUGGGUAUAUCUAA, CUUUACAGCUCGGAUUUAU), or 187.5nM control siRNA (MISSION Universal Negative Control #1) (all from Sigma-Aldrich) by using Superfect (Qiagen) per the manufacturer's instructions. Human cells were transfected with 37.5 pM control siRNA or Peli1 siRNA (Santa Cruz Biotechnology) per the manufacturer's instructions. Transfected cells were grown in RPMI medium containing 10% FBS. QPCR analysis of Peli1mRNA was used to confirm the effects of the siRNA knockdown. At 48 h post-infection, cells were infected with WNV with MOI of 0.1 (mouse cells) or MOI of 1 or 5 (human cells) respectively. Supernatants and cells were harvested at 24 h and 96 h pi to measure viral load and cytokine production.

Cytokine Bioplex: Analysis of cytokine production by using a Bio-Plex Pro Mouse Cytokine Assay (Bio-Rad).

.

Supplemental References:

57. Park EK, Jung HS, Yang HI, Yoo MC, Kim C, and Kim KS. Optimized THP-1 differentiation is required for the detection of responses to weak stimuli. *Inflamm Res.* 2007;56(1):45-50.

58. Wu P, Tarasenko YI, Gu Y, Huang LY, Coggeshall RE, and Yu Y. Region-specific generation of cholinergic neurons from fetal human neural stem cells grafted in adult rat. *Nature neuroscience.* 2002;5(12):1271-8.

59. Brien JD, Uhrlaub JL, and Nikolich-Zugich J. West Nile virus-specific CD4 T cells exhibit direct antiviral cytokine secretion and cytotoxicity and are sufficient for antiviral protection. *J Immunol.* 2008;181(12):8568-75.

60. Brien JD, Uhrlaub JL, and Nikolich-Zugich J. Protective capacity and epitope specificity of CD8(+) T cells responding to lethal West Nile virus infection. *Eur J Immunol.* 2007;37(7):1855-63.

61. Purtha WE, Myers N, Mitaksov V, Sitati E, Connolly J, Fremont DH, et al. Antigen-specific cytotoxic T lymphocytes protect against lethal West Nile virus encephalitis. *Eur J Immunol.* 2007;37(7):1845-54.

62. Wang S, Welte T, McGargill M, Town T, Thompson J, Anderson JF, et al. Drak2 contributes to West Nile virus entry into the brain and lethal encephalitis. *J Immunol.* 2008;181(3):2084-91.